

UNIVERSITY OF KWAZULU-NATAL



**A NEW AUTOMATIC REPEAT REQUEST PROTOCOL BASED ON
ALAMOUTI SPACE-TIME BLOCK CODE OVER RAYLEIGH FADING
CHANNELS**

By

Muzi Lubisi

Supervised by:

Prof. Hongjun Xu

A thesis submitted in fulfilment for the degree of Master of Science in Engineering

In the

Disipline of Electrical, Electronic and Computer Engineering,

College of Agriculture, Engineering and Science,

University of KwaZulu-Natal, Durban, South Africa

December 2020

CERTIFICATION

As the candidate's Supervisor, I agree to the submission of this dissertation.

Signed: Prof. Hongjun Xu

Date: December 2020

DECLARATION - PLAGIARISM

I, Muzi Lubisi declare that:

1. The research reported in this dissertation, except where otherwise indicated, and is my original research.
2. This dissertation has not been submitted for any degree or examination at any other university.
3. This dissertation does not contain other persons' data, pictures, graphs or other information, unless specifically acknowledged as being sourced from other persons.
4. This dissertation does not contain other persons' writing, unless specifically acknowledged as being sourced from other researchers. Where other written sources have been quoted, then:
 - a) Their words have been re-written, but the general information attributed to them has been referenced
 - b) Where their exact words have been used, then their writing has been placed in italics and inside quotation marks and referenced.
 - c) This dissertation does not contain texts, graphics or tables copied and pasted from the internet, unless specifically acknowledged, and the source being detailed in the thesis and in the Reference section.

Signed: Muzi Lubisi

Date: December 2020

ACKNOWLEDGEMENTS

My deepest appreciation goes to Professor Hongjun Xu, my supervisor, for his motivation, professional support, and guidance. I have gained a lot of knowledge concerning academic writing, study, and dedication from him. My appreciation goes to my family too; without their gracious presence, this project would not be achievable. Lastly, I would like to acknowledge my sponsor, the Armaments Corporation of South African (ARMSCO), for their financial assistance and the motivation to further strengthen myself. Appreciation be to the Creator.

“Any innovation is from replication...”

~Prof. Hongjun Xu

DEDICATION

This dissertation is dedicated to my mother Maria Nomvula Lubisi, my sister Zodwa Sibiya, my brother Sifiso Lubisi, my grandmother Sarah Sambo, my late granddaddy Elfias Lubisi may his Soul Rest in Peace and finally to my family and friends.

ABSTRACT

Spatial and multiplexing diversity of multiple-input multiple-output (MIMO) schemes improves link reliability and data rates of wireless networks. MIMO-based space-time block codes (STBCs) improve wireless network reliability by using different copies of the receiver's original data. Recently automatic repeat request (ARQ) technique was introduced for MIMO schemes to enhance the system's link reliability. ARQ improves the link reliability by using acknowledgments and timeouts to ensure efficient transmission of data over an insecure system.

In this dissertation, we propose a new ARQ protocol based on Alamouti space-time block code (STBC) over Rayleigh fading channels. The proposed system transmits data by employing two transmit antennas ($N_T = 2$) and four receive antennas ($N_R = 4$), and it is developed by applying the recent technique called uncoded space-time labeling diversity (USTLD). The main idea behind the proposed technique is to use two distinct mappers to improve the error performance of the system. The theoretical expression of the proposed technique is derived employing the union bound approach, and the theoretical analysis is validated with the simulation results.

Furthermore, the results revealed that there is a symbol error probability (SEP) performance improvement of 4 dB for 16-QAM and 4.90 dB for 64-QAM when one mapper is employed as compared to the Alamouti system at a SEP of 10^{-5} . The results also revealed that when the proposed system uses two mappers, there is a SEP performance improvement of 7.98 dB for 16-QAM and 9.8 dB for 64-QAM compared to the Alamouti system at a SEP of 10^{-5} .

TABLE OF CONTENTS

CERTIFICATION	i
DECLARATION - PLAGIARISM	ii
ACKNOWLEDGEMENTS	iii
DEDICATION	iv
ABSTRACT	v
LIST OF FIGURES	ix
LIST OF TABLES	x
LIST OF ACROYNMS	xi
LIST OF SYMBOLS	xv
CHAPTER 1.....	1
Research Background	1
1.1 Introduction.....	1
1.2 Key Wireless Technologies Used in This Dissertation	2
1.2.1 MIMO Schemes	2
1.2.2 The Alamouti System	4
1.2.3 The ARQ Protocol	5
1.2.4 Uncoded Space-Time Labeling Diversity	5
1.3 Research Motivation and Problem Statement.....	6
1.4 Research Objectives	7
1.5 Organization of Dissertation	8
1.6 Notation	8
CHAPTER 2.....	9
Alamouti Transmission with Automatic Repeat Request Protocol	9

2.1 Introduction.....	9
2.2 System model.....	10
2.3 Error Performance Analysis.....	13
2.3.1 Theoretical Analysis of	13
2.3.2 Theoretical Analysis of	14
2.4 Numerical Results.....	14
2.5 Conclusion	16
CHAPTER 3.....	17
The Uncoded Space-Time Labeling Diversity.....	17
3.1 Introduction.....	17
3.2 System Model.....	18
3.3 Error Performance Analysis.....	19
3.4 Numerical Results.....	19
3.5 Conclusion	21
CHAPTER 4.....	22
A New Automatic Repeat Request Protocol Based on Alamouti Space-Time Block Code over Rayleigh Fading Channels	22
4.1 Introduction.....	22
4.2 Proposed System Model	24
4.3 Error Performance Analysis.....	27
4.3.1 Theoretical Analysis of P_a	28
4.3.2 Theoretical Analysis of P_b	28
4.4 Numerical Results	32
4.5 Conclusion.....	34
CHAPTER 5.....	36
Conclusion and Future Research	36

5.1 Concluding Remarks	36
5.2 Future Research	37
APPENDIX A.....	39
REFERENCES	41

LIST OF FIGURES

Figure 1.1: MIMO communication scheme.....	3
Figure 1.2: Alamouti system.....	4
Figure 2.1: SEP performance of the ARQ protocol for 16-QAM, over different number of transmissions.....	15
Figure 2.2: SEP performance of the ARQ protocol for 64-QAM, over different number of transmissions.....	16
Figure 3.1: 4×2 16-QAM BER performance of the USTLD system.....	20
Figure 3.2: 4×2 64-QAM BER performance of the USTLD system.....	20
Figure 4.1: Proposed system model.....	24
Figure 4.2: 4×2 16-QAM comparison of the proposed system and the Alamouti system.....	33
Figure 4.3: 4×2 64-QAM comparison of the proposed system and the Alamouti sytem.....	33
Figure A.1: 16-QAM Gray-coded labelling map (ω^1).....	38
Figure A.2: 16-QAM optimized labelling map (ω^2).....	38
Figure A.3: 64-QAM Gray-coded labelling map (ω^1).....	39
Figure A.4: 64-QAM optimized labelling map (ω^2).....	39

LIST OF TABLES

Table 5.1: Summarized error performance gains of different number of transmission (N and 2) for various modulation schemes and orders.....	36
---	----

LIST OF ACROYNMS

ABEP.....	Average Bit Error Probability
ACK.....	Acknowledgment
AWGN.....	Additive White Gaussian Noise
ARQ.....	Automatic Repeat Request
BE.....	Bit Error
BEP.....	Bit Error Probability
BER.....	Bit Error Rate
BI-STCM.....	Bit-Interleaved Space-Time Coded Modulation
BLAST.....	Bell-Labs Layered Space-Time
CR.....	Constellation Rearrangement
CSI.....	Channel State Information
dB.....	Decibel
DMT.....	Diversity Multiplexing Tradeoff
DSTBC.....	Differential Space-Time Block Code
EP.....	Error Probability
FEC.....	Forward-Error-Correction

FER.....	Frame Error Rate
GSMC.....	Global System for Mobile Communication
HARQ.....	Hybrid Automatic Repeat Request
HDLC.....	Higher-Level Data Link Control
ICI.....	Inter-Channel Interference
i.i.d.....	Independent and Identically Distributed
ISI.....	Inter-Symbol Interference
LC.....	Low-Complexity
LD.....	Linear-Decoding
LD.....	Labeling Diversity
LTE.....	Long Term Evolution
MbM.....	Media-Based Modulation
MGF.....	Moment Generating Function
MIMO.....	Multiple-Input Multiple-Output
MIMO-ARQ.....	Multiple-Input Multiple-output-Automatic Repeat Request
MISO.....	Multiple-Input Single-Output
ML.....	Maximum-Likelihood

M-PSK.....	M-ary Phase Shift Keying
M-QAM.....	M-ary Quadrature Amplitude Modulation
MRC.....	Maximum Ratio Combining
PDF.....	Probability Density Function
PEP.....	Pairwise Error Probability
PER.....	Packet Error Rate
PSK.....	Phase Shift Keying
QAM.....	Quadrature Amplitude Modulation
RF.....	Radio Frequency
RV.....	Random Variable
SC.....	Selection Combining
SEP.....	Symbol Error Probability
SER.....	Symbol Error Rate
SISO.....	Single-Input Single-Output
SM.....	Spatial Modulation
SNR.....	Signal-to-Noise Ratio
STBC.....	Space-time Block Code

STBC-SM-LD.....Space-Time Block Coded Spatial Modulation with Labelling Diversity

STC..... Space-Time Coding

STLD.....Space-Time Labeling Diversity

STTC.....Space-Time Trellis Coding

SR.....Selective-Repeat

TCM.....Trellis-Coded Modulation

TCP.....Transmission Control Protocol

USTLD.....Uncoded Space-time Labelling Diversity

V-BLAST.....Vertical-Bell Laboratories Layered Space-Time Architecture

ZF.....Zero Forcing

WiFi.....Wireless Fidelity

WiMAX.....Worldwide Interoperability for Microwave Access

WLAN.....Wireless Local Area Network

3G.....Third Generation

5G.....Fifth Generation

LIST OF SYMBOLS

y	The scalar value of y .
\mathbf{y}	Vector of \mathbf{y} .
$ y $	The modulus of y .
\mathbf{y}^T	Transpose of \mathbf{y} .
\mathbf{y}^H	Hermitian of \mathbf{y} .
$\ \mathbf{y}\ _F$	Frobenius norm of \mathbf{y} .
$E[Y]$	The statistical expectation of Y .
$\operatorname{argmin}\{f(y)\}$	Value of y minimizing the function $f(y)$.
N_R	Number of arbitrary receive antennas.
N_T	Number of arbitrary transmit antennas.
\geq	Greater than or equal to.
\cong	Approximately equal to.
$N(\mu, \sigma^2)$	Normal Gaussian distribution with mean μ and variance σ^2 .
$\exp(y)$	Exponential function of y .
$\mathbb{C}^{(N_R \times N_T)}$	A set of $N_R \times N_T$ complex-valued matrices.

CHAPTER 1

Research Background

1.1 Introduction

In wireless communication systems, data rates and/or link reliability are often enhanced by employing multiple-input multiple-output (MIMO) technique [1]. MIMO systems achieve this by offering spatial multiplexing, spatial diversity, or a trade-off of both. Spatial multiplexing is accomplished with independent codewords sent to the receiver simultaneously, with the aim of improving data rates of wireless networks. On the other hand, spatial diversity is realized by transmitting redundant codewords to the receiver to enhance link reliability [2].

The Alamouti space-time block code (STBC) is one type of two input MIMO system [3]. It transmits data by employing two transmit antennas during two time slots. However, only full-diversity and no multiplexing gain is accomplished by the Alamouti STBC [4]. The link reliability in the Alamouti system is achieved by transmitting redundant duplicates of the original symbol to the receiver through two transmit antennas. Signals are transmitted to the receiver across different channels paths and at different times. The received signals are combined in an optimal manner at the receiver to reconstruct the initial signals.

Reliability can be further improved in a wireless communication system by using diversity techniques. Diversity approaches are employed to reduce the effect of channel fading on wireless networks and thus improve the reliability between transmitter and receiver. [5]. This dissertation focuses on spatial diversity and labeling diversity.

Spatial or space diversity is achieved by implementing a multiple transmit and receive antenna MIMO technique thus; multiple paths are established between the transmitter and the receiver [6]. This approach offers significant error performance improvement without compromising the vital bandwidth on the energy resources transmitted. Spatial diversity is commonly applied as it is easy to deploy and very economical. In order to prevent the

correlation among the signals received from each received antenna, the spatial positions for receive antennas are separated sufficiently [5]. The usual separation between the receive antennas is a few wavelengths of the transmitted signal. Each received signal is combined to increase its overall signal-to-noise ratio (SNR) by using selection combining (SC) or maximal ratio combination (MRC), which thus mitigates the effects of fading.

Labeling diversity was initially introduced with iterative decoding to a bit-interleaved coded system [7]. However, in such systems, the use of convolutionary encoding and decoding techniques causes high detection complexity, leading to higher memory consumption. This has led to studies, which apply labeling diversity to uncoded systems, which are typically more cost-effective and more straightforward to implement. Examples of these uncoded systems are: (i) multi-packets with automatic repeat requests for data transmissions [8] and (ii) decode-and-forward relay systems [9].

In labeling diversity, the same information is encoded before transmission with different bit-to-symbol mappers. The mappers are constructed so that each mapper can map the symbol that corresponds to a given label [10]. Each label is therefore represented as a point in a dimensional hyperspace for a labeling diversity scheme that uses x mappers. The purpose of the mapper configuration in this hyperspace is to maximize the distance between points that correspond to each label [10]. Each mapper's constellation would then literally be a plane inside the dimensional space.

A summary of the key wireless technologies used in this dissertation is provided in the sections below.

1.2 Key Wireless Technologies Used in This Dissertation

This section briefly presents the wireless technologies used in this dissertation.

1.2.1 MIMO Schemes

MIMO wireless networking techniques have become popular and have been introduced into evolving broadband access technologies such as 5G (fifth generation) and LTE (long-term evolution). More capacity is required as mobile data traffic keeps increasing. When more transmit or receive antennas are mounted, the more potential signal paths, the better the

transmission range, and the more reliable the connection [1]. There are, however, drawbacks such as increasing hardware complexity and power usage at both ends of signal processing.

The MIMO system comprises multiple antennas for enhancing link reliability at the transmitter and receiver ends, as displayed in Figure 1.1. The benefits of MIMO schemes are increased capacity, transmission range, and robustness, such that multiple data streams are permitted. In [1], MIMO systems are classified into three groups according to their transmission techniques, namely spatial multiplexing, diversity coding, and precoding.

Spatial multiplexing is a wireless MIMO multiplexing approach used to transmit independent space-separated channels [11]. The basic feature of spatial multiplexing technique is to transform the data streams into separate streams of data. Hence, this improves the link reliability by transmitting many independent streams over multiple antennas.

In diversity coding, the transmitter needs no information of channel state information (CSI) when a single stream of data is transmitted; however, the transmitted signal is configured by an approach known as space-time coding before transmission [12]. The variation of the channel in time, frequency, and space with multiple copies of data arriving at the receiver can be defined as diversity. The amount of improvement that can be achieved in terms of the received signal (in diversity scheme) relies on the fading characteristics of the signal being transmitted [12]. This technique utilizes the independent fading of the channel to improve the reliability of the system.

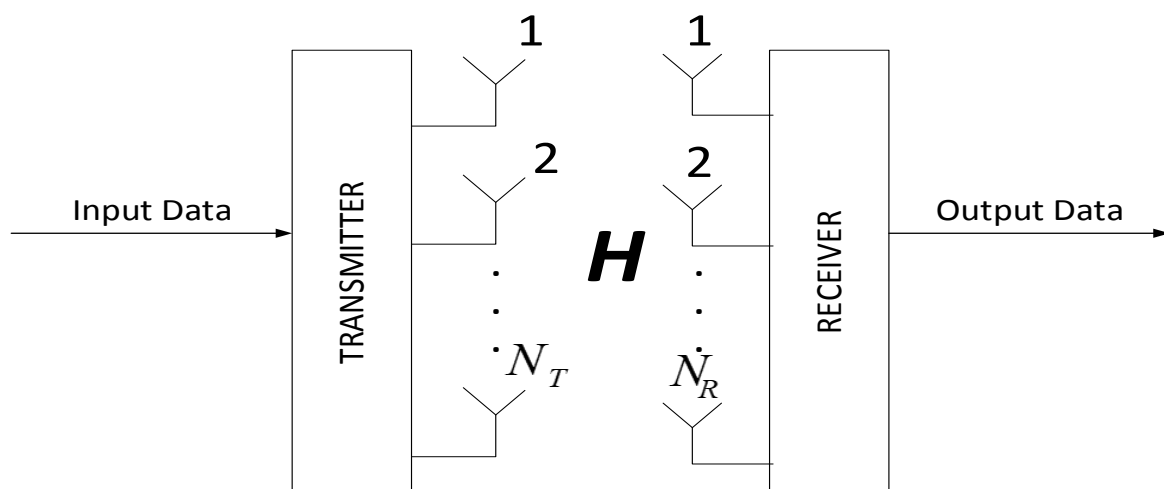


Figure 1.1: MIMO communication scheme [13].

Precoding is a type of transmit diversity technique which sends out pre-coded information to the receiver according to the known CSI, employing multi-stream beamforming [14]. The CSI is attained over a relatively large time for a fixed channel or for an evenly distributed channel. If there is CSI on the transmitter side, the signals transmitted are divided on the transmitter by pre-equalization. Signals are transmitted at the required phase and amplitude at each of the available transmit antennas [14].

1.2.2 The Alamouti System

Alamouti introduced the first form of space-time block coding in 1998 [3]. Alamouti scheme is a space-time block coding technique [3]. The Alamouti system achieve full diversity ($2N_R$), where N_R is the number of receiving antennas. The Alamouti scheme also has a simple linear detection algorithm since the Alamouti codeword matrix is orthogonal [3, 4].

The Alamouti system transmits data by employing two transmit antennas and two time slots. As shown in [3], the Alamouti scheme is similar to a $1 \times 2N_R$ MRC scheme with a 3dB loss. The Alamouti STBC system is illustrated in Figure 1.2.

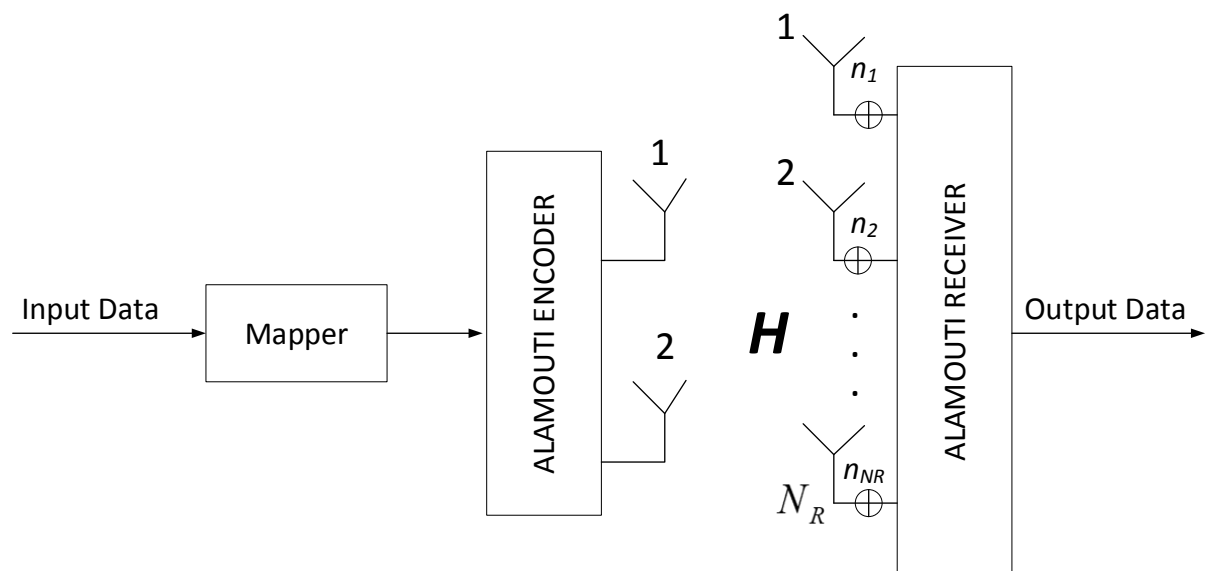


Figure 1.2: The Alamouti system [3].

The modulated symbol pairs are transmitted over quasi-static Rayleigh fading channels. The transmission matrix also known as the Alamouti STBC is defined by [3]:

$$\mathbf{s}_{Alamouti} = \begin{bmatrix} s_1 & s_2 \\ -s_2^* & s_1^* \end{bmatrix}. \quad (1.1)$$

In (1.1), the rows denote time slot one and time slot two, and the columns denote the modulated signals conveyed from antenna one and antenna two in a given time slot. The signals that are transmitted are decoupled at the receiver, since the codeword matrix of the Alamouti system is orthogonal. The orthogonality of Alamouti STBC is exploited for low-complexity (LC) linear decoding [15].

1.2.3 The ARQ Protocol

Transmission errors are introduced by transmitting data over a channel; hence, such errors decrease the reliability of the system. Therefore, error management should be performed to build a system with reduced errors to combat errors that occur. Error management usually includes the data link layer and error management systems such as automatic repeat request (ARQ) [16].

The ARQ is an error management protocol, which automatically activates a demand for retransmission of data streams once the incorrect or faulty data is received. If a confirmation signal to confirm receiving of data is missing from the transmitter system, the transmission of the data is normally retransmitted after a prescribed period and the procedure is repeated until the acknowledgment is obtained in the transmitting system [17]. ARQs are utilized to deliver secure transmissions through untrustworthy upper layer services. They are commonly utilized in global system for mobile communication (GSMC).

1.2.4 Uncoded Space-Time Labeling Diversity

The uncoded space-time labeling diversity (USTLD) is a space-time block code scheme with two transmit antennas, proposed by Xu et al. [10]. The USTLD system attains an improved error performance over the Alamouti STBC system [10]. USTLD accomplishes labeling diversity by employing two labeling maps to map the binary streams to symbols.

The USTLD scheme transmit a mapped symbol pair in two time-slots [18]. The USTLD matrix is not an orthogonal transmission matrix, unlike the Alamouti system. Consequently, there is a higher complexity detection on the USTLD receiver since the joint ML detector detects all possible symbol pairs compared to the Alamouti system.

In this dissertation, USTLD will be employed to enhance the error performance of the proposed system. The USTLD technique will be applied to an ARQ protocol to create a new system. The details of USTLD are presented in Chapter 3.

1.3 Research Motivation and Problem Statement

In this section, the motivation of this dissertation and the objectives of the research are highlighted. Research carried out over the last decade has shown that the use of MIMO systems offers a significant link reliability and diversity gain [19, 20].

MIMO schemes have several disadvantages including high inter-channel interference (ICI), high proportion of radio frequency (RF) chains, high complexity of decoding due to ICI, high-energy efficiency and increased hardware costs because of multiple parallel transmitters and receivers [1]. There is also a trade-off regarding improved reliability and data rates. Additional channel error protection is thus, required for the signal transmitted. Error management systems are used with additional robustness to improve the system's error performance [21]. The proposed system employs the ARQ protocol as an approach for error control. Hence, it is necessary to analyze the existence of the MIMO channels in the presence of ARQ protocols.

MIMO-ARQ systems have been previously developed to improve the error performance of wireless communication networks [16, 22, 23, 24]. In [16], the error performance of MIMO systems in with ARQ has been investigated. However, [16] did not compare the different number of retransmission, the results were concerned with implications of time-varying signal power, MIMO-ARQ broad scale and data transmission models, but this was remedied in [22, 23], where the different number of retransmissions were compared. This motivates an investigation of different number of retransmissions in MIMO systems with ARQ protocol.

Similarly, MIMO-ARQ proposed in [24, 25] investigated a technique for enhancing diversity among packet retransmissions by symbol mapping for systems that employs modulation schemes such as QAM and PSK in AWGN and fading channels. Labeling diversity is called mapping diversity in both systems in [24, 25]. The diversity between M retransmissions has been enhanced by adjusting the symbol mapping for every transmission. It was also noted

that four transmit and four receive antennas were used in both techniques in [24, 25]. In addition, the study in [25], investigated mapping diversity on incoherent and coherent decoding with signal space diversity in flat fading channels. However, the proposed system does not employ flat-fading channels with coherent and incoherent and demodulation. This motivates an investigation of mapping diversity or labeling diversity in MIMO-ARQ systems over quasi-static Rayleigh fading channels.

MIMO-ARQ systems with Alamouti STBC can exhibit significant improvement when compared to a conventional MIMO system of the same assumptions [26]. Additionally, Alamouti STBC has been stated in the literature that it can further improve the error performance of an ARQ system by employing two transmit antennas. As investigated in [26], which demonstrates that the incorporation of Alamouti STBC in a MIMO-ARQ system can further improve the error performance and ARQ is employed to enhance the link reliability.

In this dissertation, we propose an ARQ protocol in MIMO systems based on Alamouti STBC that employs labeling diversity. The proposed system is known as a new ARQ protocol based on Alamouti space-time block code over Rayleigh fading channels.

In [25], the bit error probability of symbol mapping for packet retransmission via fading channels was derived using union bound, which does not match very well at the low SNR region. In [26], the frame error probability was evaluated for Rayleigh fading channels using an upper bound approach of two-user cooperative ARQ technique. Result shows that the approach in [26] matches very closely at lower SNR validating the results from low SNR to high SNR region than the method used in [25], which employs a union bound. This motivates for the formulation of the theoretical analysis of the proposed system to validate the simulation results.

1.4 Research Objectives

The following are the objectives of this research:

- Formulation of the analytical expression for ARQ protocol and validate it with simulation results.

- Compare the first transmission and the second transmission with and without labeling diversity.
- Formulation of the symbol error probability for the proposed system by employing the upper bound approach.

1.5 Organization of Dissertation

The rest of this dissertation is presented as follows:

- Chapter 2 carries out a detailed overview of Alamouti transmission with ARQ protocol, along with numerical results.
- Chapter 3 provides the USTLD system model with the theoretical error performance, employing the union bound technique in frequency-flat Rayleigh fading channels and confirm the validity of the Monte Carlo simulation results.
- Chapter 4 presents the proposed ARQ protocol based on Alamouti STBC over Rayleigh fading channels. Chapter 4 further derives the proposed scheme's theoretical error performance over independent and identically distributed (i.i.d) quasi-static Rayleigh fading channels. Thereafter, it provides the simulation and theoretical results for the proposed system and compares these results with the Alamouti system under the same channels and AWGN conditions.
- Chapter 5 summarizes the dissertation and explores potential future directions for the investigation.

1.6 Notation

Bold italics symbols denote matrices or vectors however, normal letters are scalar. $|\cdot|$, $(\cdot)^H$, $[\cdot]^T$, $\|\cdot\|_F$, and $\max\{\cdot\}$ denote the Euclidean norm, Hermitian, transpose, Frobenius norm, and complex conjugate of a number. $Q(\cdot)$ denote the Gaussian Q-function, $Re\{\cdot\}$ is the real part of a complex value, whereas $Im\{\cdot\}$ is the imaginary part of a complex value and $E\{\cdot\}$ is the expectation operator. $\max\{\cdot\}$ denote the maximum value of the argument for x . N_T and N_R represent the number of transmit and receive antennas.

CHAPTER 2

Alamouti Transmission with Automatic Repeat Request Protocol

2.1 Introduction

Multiple-input multiple-output (MIMO) based communications schemes have significantly improved reliability and data rates in wireless systems over the past few decades compared to single-input single-output (SISO) schemes [1]. The reliability of MIMO systems can be improved by combining it with an ARQ technique, which lessens communication system errors. MIMO based automatic repeat request (MIMO-ARQ) systems improve reliability by retransmitting the same information bits for different number of transmissions to reduce errors in communication systems. Over the past few years, MIMO-ARQ systems have developed a significant attention in the research community because of their diversity-multiplexing trade-off [17].

ARQ systems have been configured to assume linear transmission through a channel [27]. In the ARQ schemes, if errors occur during error detection when a data packet is being processed an error is reported, and a demand for transmission is made. A number of studies have been reported for combining packets and producing diversity between retransmission systems equipped with the ARQ technique [8]. For instance, Chase has established an ARQ system that employs maximum likelihood for specific packet numbers [28]. The authors in [29] suggested ARQ methods, such as a strategy in which soft-decoded codewords are merged in a single soft codeword in the multiple packet transmission. Others have established systems that are associated with rate-compatible codes, such as Rowitch et al. [30] and Hagenauer [31], where the duplicates being transmitted of the packet is fractured so that reliability is improved. Stuber and Narayanan have created a turbo-code ARQ receiver for reuse of the extrinsic data from previous packets. The work in [16] has

developed diversity strategies generated by inter-symbol interference (ISI) channels retransmissions.

This chapter aims to address the Alamouti transmission with ARQ protocol for schemes that employ quadrature amplitude modulation (QAM) over Rayleigh fading channels. Additionally, we establish a theoretical error analysis for N transmissions over Rayleigh fading channels.

2.2 System model

We consider the case whereby we have N retransmission for the ARQ protocol, where N is the maximum number of retransmissions. The transmission is based on frames, where each frame has a length of $2N_o$ symbols and N_o is the maximum number of symbols in a frame.

We focus for $N = 1$ and $N = 2$ number of transmissions. When $N = 1$, for the first frame consider an $N_R \times N_T$ MIMO scheme with $N_T = 2$ transmit antennas and N_R receive antennas. Initially, two binary streams $\boldsymbol{\delta}_1 = [\delta_{1,1} \delta_{1,2} \dots \delta_{1,m}]$ and $\boldsymbol{\delta}_2 = [\delta_{2,1} \delta_{2,2} \dots \delta_{2,m}]$, each of length $m = \log_2 M$ are fed into a Gray-coded mapper ($\boldsymbol{\Omega}$) which maps m bits into an M-QAM constellation point and yields symbols s_1 and s_2 . Each symbol is normalized such that $E\{|s_1|^2\} = E\{|s_2|^2\} = 1$. The Alamouti STBC encoder matrix is defined by:

$$\mathbf{S}_{Alam} = \begin{bmatrix} s_1 & s_2 \\ -s_2^* & s_1^* \end{bmatrix}. \quad (2.1)$$

At time slot one, the first and second antenna concurrently transmit symbols s_1 and s_2 . At time slot two, the first and second antenna concurrently transmit symbols $-s_2^*$ and s_1^* , respectively. The received signal vectors are given by

$$\mathbf{y}_1 = \sqrt{\frac{E_s}{2}} (\mathbf{h}_1 s_1 + \mathbf{h}_2 s_2) + \mathbf{n}_1, \quad (2.2)$$

$$\mathbf{y}_2 = \sqrt{\frac{E_s}{2}} (-\mathbf{h}_1 s_2^* + \mathbf{h}_2 s_1^*) + \mathbf{n}_2, \quad (2.3)$$

where $\mathbf{y}_\ell \in \mathbb{C}^{N_R \times 1}$ is the ℓ^{th} received signal vector, for $\ell \in [1:2]$, E_s signifies the average signal-to-noise ratio (SNR) of transmission. $\mathbf{n}_\ell \in \mathbb{C}^{(N_R \times 1)}$ and $\mathbf{h}_\ell \in \mathbb{C}^{(N_R \times 1)}$ signifies the ℓ^{th} additive white Gaussian noise (AWGN) vector and the fading channel vector for $\ell \in [1:2]$. The complex entries of \mathbf{h}_ℓ and \mathbf{n}_ℓ are independent and identically distributed (i.i.d) Gaussian

random variables (RVs) distributed as $CN(0,1)$. In addition, it is assumed that each entry of \mathbf{h}_ℓ is quasi-static Rayleigh fading [15]. The channel remains the same value in two-time slots and takes an independent value in another two-time slots.

Based on [3, 32], it is assumed that full channel state information (CSI) is known at the receiver. The received signals in (2.2) and (2.3) are sent to the combiner and the output of the combiner is given by:

$$r_1 = (\mathbf{h}_1^H)(\mathbf{y}_1) + (\mathbf{y}_2^H)(\mathbf{h}_2) = g_1 s_1 + \tilde{n}_1, \quad (2.4)$$

$$r_2 = (\mathbf{h}_2^H)(\mathbf{y}_1) - (\mathbf{y}_2^H)(\mathbf{h}_1) = g_1 s_2 + \tilde{n}_2, \quad (2.5)$$

where $g_1 = \sqrt{\frac{E_s}{2}}(\|\mathbf{h}_1\|_F^2 + \|\mathbf{h}_2\|_F^2)$, $\tilde{n}_1 = \mathbf{h}_1^H \mathbf{n}_1 + \mathbf{n}_2^H \mathbf{h}_2$ and $\tilde{n}_2 = \mathbf{h}_2^H \mathbf{n}_1 - \mathbf{n}_2^H \mathbf{h}_1$ [33].

Equation (2.4 – 2.5) can be further expressed by

$$r_i = g_1 s_i + \tilde{n}_i ; i \in [1:2], \quad (2.6)$$

Therefore, the estimation of the M-QAM symbols is done by minimizing the ML metric expressed as:

$$\hat{s}_1 = \operatorname{argmin}_{s_1 \in \chi} (|r_1 - s_1|^2), \quad (2.7)$$

$$\hat{s}_2 = \operatorname{argmin}_{s_2 \in \chi} (|r_2 - s_2|^2), \quad (2.8)$$

where χ is a set containing all the possible modulated symbols such that $s_1, s_2 \in \chi$.

If there are errors in the first frame for $2N_o$ symbols after detection, previous erroneous transmissions will be saved to the data buffer to minimize current transmission errors, typically by combining the ML detection of recent transmission. The transmitter will request a new transmission by transmitting the same symbols as from the first transmission. Only the fading channel and AWGN noise will differ from the first transmission. Then for the second frame the $N_R \times 1$ received signal vector for the second transmission ($N = 2$) is given by

$$\mathbf{y}_3 = \sqrt{\frac{E_s}{2}}(\mathbf{h}_3 s_1 + \mathbf{h}_4 s_2) + \mathbf{n}_3, \quad (2.9)$$

$$\mathbf{y}_4 = \sqrt{\frac{E_s}{2}}(-\mathbf{h}_3 s_2^* + \mathbf{h}_4 s_1^*) + \mathbf{n}_4, \quad (2.10)$$

where $\mathbf{y}_{\ell+2} \in \mathbb{C}^{N_R \times 1}$ is the ℓ^{th} received signal vector, for $\ell \in [1:2]$, E_s signifies the average SNR of transmission. $\mathbf{h}_{\ell+2} \in \mathbb{C}^{(N_R \times 1)}$ and $\mathbf{n}_{\ell+2} \in \mathbb{C}^{(N_R \times 1)}$ signifies the ℓ^{th} fading channel vector and AWGN vector for $\ell \in [1:2]$. The complex entries of $\mathbf{h}_{\ell+2}$ and $\mathbf{n}_{\ell+2}$ are i.i.d Gaussian RVs distributed as $CN(0,1)$. In addition, it is assumed that each entry of $\mathbf{h}_{\ell+2}$ is quasi-static Rayleigh fading [15]. The channel remains the same value in two-time slots and takes an independent value in another two-time slots.

Based on [3, 32], it is assumed that CSI is known at the receiver. The received signals in (2.9) and (2.10) are sent to the combiner and the output of the combiner is given by:

$$r_3 = (\mathbf{h}_3^H)(\mathbf{y}_3) + (\mathbf{y}_4^H)(\mathbf{h}_4) = g_2 s_1 + \hat{n}_1, \quad (2.11)$$

$$r_4 = (\mathbf{h}_4^H)(\mathbf{y}_3) - (\mathbf{y}_4^H)(\mathbf{h}_3) = g_2 s_2 + \hat{n}_2. \quad (2.12)$$

where $g_2 = \sqrt{\frac{E_s}{2}}(\|\mathbf{h}_3\|_F^2 + \|\mathbf{h}_4\|_F^2)$, $\hat{n}_1 = \mathbf{h}_3^H \mathbf{n}_3 + \mathbf{n}_4^H \mathbf{h}_4$ and $\hat{n}_2 = \mathbf{h}_4^H \mathbf{n}_3 - \mathbf{n}_4^H \mathbf{h}_3$ [33].

Equation (2.11 – 2.12) can be further expressed by

$$r_{i+2} = g_2 s_i + \hat{n}_i ; i \in [1:2], \quad (2.13)$$

Since the first transmission and the second transmission transmit the same symbols, the equivalent model for the second transmission can be combined with that of the first transmission given by

$$\mu_i = v_i + v_{i+2} = (g_1 s_i + \tilde{n}_i) + (g_2 s_i + \hat{n}_i). \quad (2.14)$$

Equation (2.14) may be further simplified as:

$$\mu_i = (g_1 + g_2) s_i + \bar{n}_i ; i \in [1:2], \quad (2.15)$$

where $\bar{n}_i = \tilde{n}_i + \hat{n}_i ; i \in [1:2]$.

Finally, the estimation of the M-QAM symbols is done by minimizing the ML metric expressed as:

$$\tilde{s}_1 = \operatorname{argmin}_{s_1 \in \mathcal{X}} (|\mu_1 - s_1|^2), \quad (2.16)$$

$$\tilde{s}_2 = \operatorname{argmin}_{s_2 \in \chi} (|\mu_2 - s_2|^2), \quad (2.17)$$

where χ is a set containing all the possible modulated symbols such that $s_1, s_2 \in \chi$.

2.3 Error Performance Analysis

In this section, we derive the error performance for the ARQ protocol. The overall error probability for the protocol is expressed as

$$P_e = P_{SEP(N=1)} \times (1 - P_{e(\text{frame error})}) + P_{SEP(N=2)} \times P_{e(\text{frame error})}, \quad (2.18)$$

where $P_{SEP(N=1)}$ is the symbol error probability for the first transmission ($N = 1$), $P_{SEP(N=2)}$ is the symbol error probability for the second transmission ($N = 2$) and $P_{e(\text{frame error})}$ is the frame error probability.

The frame error probability can be found in [27] which is expressed by

$$P_{e(\text{frame error})} = \sum_{i=1}^{N_0} \binom{N_0}{i} P_d^i (1 - P_d)^{N_0 - i}, \quad (2.19)$$

where N_0 is the maximum number of symbols in a frame and we assume that $N_0 = 100$. P_d is the symbol error probability of the symbols being successfully transmitted.

In the sections below, the symbol error probabilities are addressed separately for $P_{SEP(N=1)}$ and $P_{SEP(N=2)}$.

2.3.1 Theoretical Analysis of $P_{SEP(N=1)}$

In this section, we derive the error performance for $P_{SEP(N=1)}$, which is the theoretical analysis for the first transmission ($N = 1$); the theoretical analysis is based on (2.6). The error probability for $P_{SEP(N=1)}$ is obtained by replacing $\bar{\gamma}$ and N_R with $\frac{1}{2}\bar{\gamma}$ and $2N_R$ in the symbol error probability for maximal ratio combining (MRC), since it is the same as the error probability for Alamouti system. In [34], the Alamouti system with N_R receive antennas has been confirmed to be the equivalent to the MRC scheme with half SNR and $2N_R$ receive antennas. The conditional pairwise error probability (PEP) for MRC has been formulated in [35, 36] and is expressed as:

$$\bar{\gamma}) \left[-\left(\frac{1}{b\bar{\gamma}}\right) - \left(\frac{1}{b\bar{\gamma}+1}\right) \sum_{i=1}^N \left(\frac{i}{b\bar{\gamma}+S_i}\right) \sum_{i=1}^N \left(\frac{i}{b\bar{\gamma}+S_i}\right) \right]. \quad (2.20)$$

Therefore, the symbol error probability (SEP) for $\bar{\gamma}$, is derived by replacing $\bar{\gamma}$ and N with $-\bar{\gamma}$ and N in (2.20). Hence, (2.20) becomes

$$-\left[-\left(\frac{1}{b\bar{\gamma}+2}\right) - \left(\frac{1}{b\bar{\gamma}+1}\right) \sum_{i=1}^N \left(\frac{i}{b\bar{\gamma}+S_i}\right) \sum_{i=1}^N \left(\frac{i}{b\bar{\gamma}+S_i}\right) \right], \quad (2.21)$$

where $S_i = 2\sin^2(\frac{\pi}{4M})$, $a = 4\left(1 - \frac{1}{\sqrt{M}}\right)$, $b = \left(\frac{1}{M}\right)$, $\bar{\gamma}$ is the average SNR at each receive antenna and n is the number of iterations for $M = 10$.

2.3.2 Theoretical Analysis of

In this section, we derive the error probability of $P_{SEP(N=2)}$; the analysis is based on (2.15).

The SEP of $P_{SEP(N=2)}$ can be acquired by using $-\bar{\gamma}$ and N to replace $\bar{\gamma}$ and N_R in (2.20). Hence, (2.20) becomes

$$-\left[-\left(\frac{1}{b\bar{\gamma}+2}\right) - \left(\frac{1}{b\bar{\gamma}+1}\right) \sum_{i=1}^N \left(\frac{i}{b\bar{\gamma}+S_i}\right) \sum_{i=1}^N \left(\frac{i}{b\bar{\gamma}+S_i}\right) \right]. \quad (2.22)$$

Therefore, equation (2.21) and (2.22) are substituted into (2.18) yielding the final expression for P_e .

2.4 Numerical Results

In this section, the numerical and theoretical results for an $N_R \times N_T$ Alamouti transmission with ARQ protocol, where $N_R = 4$ and $N_T = 2$ are presented for 16-QAM and 64-QAM. This section aims to demonstrate the different transmission error performance gains and validate the analytical framework established in Section 2.3. Monte Carlo simulations have been carried out, where the SEP is plotted per receive antenna against SNR (dB). Performance comparisons for 16-QAM and 64-QAM were made at a SEP value of 10^{-5} due to the long simulation period. Simulation parameters for the channels and AWGN are in line

with those mentioned in Section 2.2. During simulation, the channel at the receiver is assumed to be known and the frame length is $2N_o$ symbols where $N_o = 100$.

The results presented in Figure 2.1 and Figure 2.2 show that the second transmission ($N = 2$) outperforms the first transmission ($N = 1$); for example, for 16-QAM there is a SEP improvement of approximately 4 dB and for 64-QAM there is a SEP improvement of approximately 4.90 dB. In addition, Figure 2.1 and Figure 2.2 also indicate that the analytical results converge with simulation results in high SNR regions in all cases.

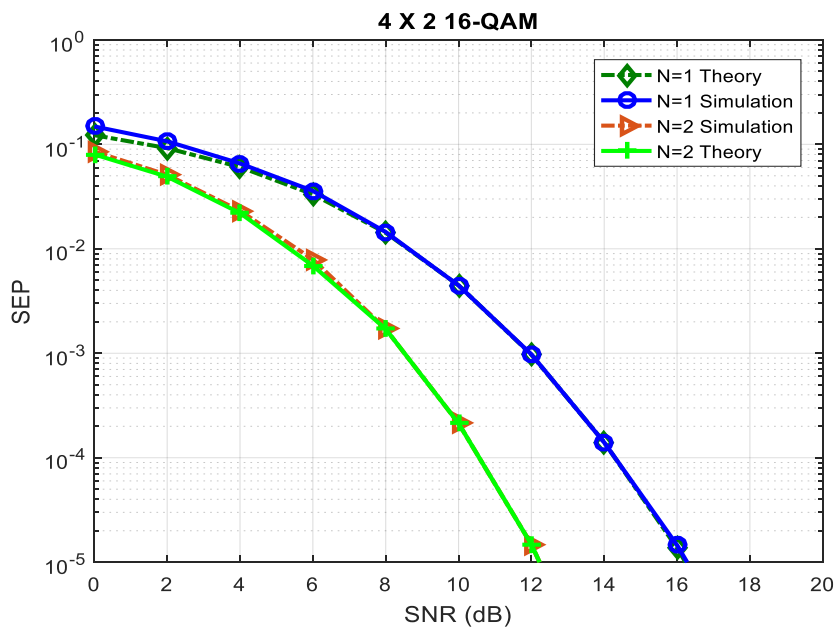


Figure 2.1 SEP performance of the ARQ protocol for 16-QAM, over different number of transmissions ($N = 1$ and $N = 2$).

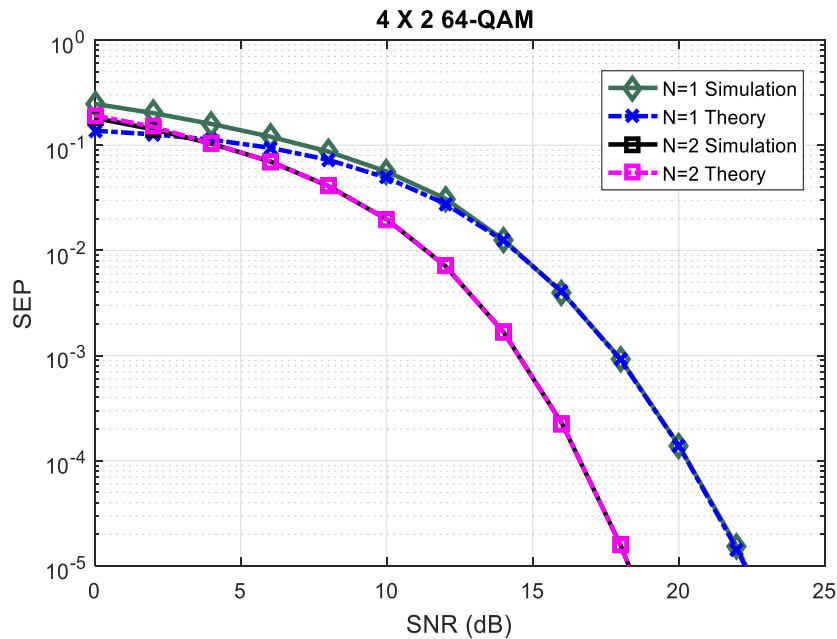


Figure 2.2 SEP performance of the ARQ protocol for 64-QAM, over different number of transmissions ($N = 1$ and $N = 2$).

2.5 Conclusion

In this chapter, the automatic repeat request protocol was presented for wireless communication systems. The ARQ system's theoretical error performance to verify the Monte Carlo simulation results over Rayleigh fading channels was formulated. The analytical results agreed well with the numerical results. Furthermore, results confirmed that the second transmission ($N = 2$) outperforms the first transmission ($N = 1$) with a SEP performance improvement of approximately 4 dB for 16-QAM and 4.90 dB for 64-QAM.

CHAPTER 3

The Uncoded Space-Time Labeling Diversity

3.1 Introduction

Space-time coded modulation (STCM) is a system commonly used in wireless communication networks, because of the reliability and data rates improvements of multiple-input multiple-output (MIMO) technologies [37]. The STCM system offers three ways of improvement in error performance namely, time diversity, antennas diversity and labeling diversity [37]. In uncoded and coded communication networks, labeling diversity has been investigated.

In uncoded communications schemes, the constellation rearrangement (CR) method of labeling diversity has been employed to enhance system error performance, using the same bit streams in multiple data transmission of packets and relay network schemes [25]. The labeling diversity design maps the bit streams into several transmission constellations and has been used in several packet transmission systems, such as wireless relay systems [9]. In [10], uncoded space-time labeling diversity (USTLD) was proposed and system has an improved error performance compared to the Alamouti system [10]. Another uncoded system proposed by Ayanda et al. [37] expanded the USTLD system introduced by Xu et al. [10] incorporating three mappers and three transmit antennas. However, in [37], they used three time-slots, thus attaining the same spectral efficiency as the existing USTLD system.

For coded schemes, study efforts to optimize asymptotic diversity gain were considered. In [38] an ideal constellation diversity approach was proposed for bit-interleaved space-time coded modulation (BI-STCM). Besides that, Huang et al. [38] introduced an enhanced 16-QAM labeling technique for BI-STCM iterative decoding utilizing Alamouti space-time block code.

In this chapter, the USTLD is presented. Additionally, the theoretical analysis for the USTLD scheme will be derived to verify the Monte Carlo simulation results.

3.2 System Model

Consider an $N_R \times N_T$ MIMO system where $N_T = 2$. Initially, two binary streams $\boldsymbol{\delta}_1 = [\delta_{1,1} \delta_{1,2} \dots \delta_{1,k}]$ and $\boldsymbol{\delta}_2 = [\delta_{2,1} \delta_{2,2} \dots \delta_{2,k}]$ each of length $k = \log_2 M$ are generated, where M is the modulation order. The USLD system uses two M-QAM mappers. Mapper 1 ($\boldsymbol{\Omega}_1^M$) follows a Gray-coded M-QAM mapper and mapper 2 ($\boldsymbol{\Omega}_2^M$) follows the optimized labelling mapper, the design of the optimized labelling mapper can be found in [10]. Initially, the binary streams $\boldsymbol{\delta}_\iota$, $\iota \in [1:2]$ are fed into mapper 1 ($\boldsymbol{\Omega}_1^M$) yielding the two symbols, $x_r^1 = \boldsymbol{\Omega}_1^M(\boldsymbol{\delta}_1)$ and $x_p^2 = \boldsymbol{\Omega}_1^M(\boldsymbol{\delta}_2)$, where $p = 1 + \sum_{\ell=1}^k 2^{k-\ell} \delta_{2,\ell}$ and $r = 1 + \sum_{\ell=1}^k 2^{k-\ell} \delta_{1,\ell}$ are symbol labels. Mapper 2 ($\boldsymbol{\Omega}_2^M$) fed the same binary streams, yielding two symbols, $\tilde{x}_r^1 = \boldsymbol{\Omega}_2^M(\boldsymbol{\delta}_1)$ and $\tilde{x}_p^2 = \boldsymbol{\Omega}_2^M(\boldsymbol{\delta}_2)$. We assume that $E\{|x_r^1|^2\} = E\{|\tilde{x}_r^1|^2\} = E\{|x_p^2|^2\} = E\{|\tilde{x}_p^2|^2\} = 1$. Let the overall USTLD codeword vector transmitted be expressed as $\mathbf{X} = [\mathbf{x}_1 \mathbf{x}_2]$, where $\mathbf{x}_1 = [x_r^1 \ x_p^2]^T$ and $\mathbf{x}_2 = [\tilde{x}_p^2 \ \tilde{x}_r^1]^T$. Therefore, the $N_R \times 1$ received signal vector is expressed by

$$\mathbf{y}_t = \sqrt{\frac{E_s}{2}} \mathbf{H}_t \mathbf{x}_t + \mathbf{n}_t; \quad t \in [1:2], \quad (3.1)$$

where $\mathbf{y}_t = [y_{1,t} \ y_{2,t} \dots \ y_{N_R,t}]^T$ signifies the received signal vector for $t \in [1:2]$, E_s signifies the average signal-to-noise ratio (SNR), \mathbf{n}_t signifies the $N_R \times 1$ additive white Gaussian noise (AWGN) vector, \mathbf{H}_t signifies the $N_R \times 2$ channel matrix defined as $\mathbf{H}_t = [\mathbf{h}_1^t \ \mathbf{h}_2^t]$, where $\mathbf{h}_\iota^t = [h_{1,\iota}^t \ h_{2,\iota}^t \dots \ h_{N_R,\iota}^t]^T$, $\iota \in [1:2]$. The complex entries of \mathbf{h}_t and \mathbf{n}_t are independent and identically distributed (i.i.d) random variables (RV) distributed as $CN(0,1)$. \mathbf{h}_t is considered to be Rayleigh frequency-flat fading channel, with channel gains remaining constant during a time slot but assuming independent values from time slot to another time slot.

Therefore, the estimation of the M-QAM symbols is done by minimizing the joint maximum likelihood (ML) metric expressed as [10]:

$$[\hat{\mathbf{x}}_1 \ \hat{\mathbf{x}}_2] = \operatorname{argmin}_{(\mathbf{x}_1, \mathbf{x}_2) \in \mathcal{X}} \left(\sum_{t=1}^2 \left\| \mathbf{y}_t - \sqrt{\frac{E_s}{2}} \mathbf{H}_t \mathbf{x}_t \right\|_F^2 \right), \quad (3.2)$$

where χ is a set containing all the possible modulated symbols such that $\chi \in \chi$.

3.3 Error Performance Analysis

The theoretical analysis in Xu et al. [10] uses the union bound to derive the error performance analysis of the USTLD system. The technique was based on the assumption that only one of the symbols is detected correctly in the symbol pairs transmitted at high SNR, while another is detected in error. Therefore, we assume x_r^1 is detected correctly, while x_p^2 is erroneously detected. The average bit error probability (ABEP) is union bounded by [10]

$$ABEP \leq \sum_{\hat{p} \neq p} P(\mathbf{X} = \hat{\mathbf{X}}), \quad (3.3)$$

where $P(\mathbf{X} = \hat{\mathbf{X}})$ is the pairwise error probability (PEP) between the transmitted codeword $\mathbf{X} = [x_p^2 \ x_r^1]$ and the received codeword $\hat{\mathbf{X}} = [\hat{x}_1 \ \hat{x}_2]$, where $\hat{x}_1 = [x_p^2 \ \tilde{x}_p^2]$ and $\hat{x}_2 = [x_r^1 \ \tilde{x}_r^1]$. \hat{x}_1 is the number of bit errors between the labels and \hat{p} , and M . The unconditional PEP has been formulated in [10] and is expressed as:

$$P(\mathbf{X} = \hat{\mathbf{X}}) = \left[-\left(\frac{1}{\bar{\gamma}}\right) \left(\frac{1}{\bar{\gamma}}\right) \sum \left(\frac{1}{\bar{\gamma}}\right) \left(\frac{1}{\bar{\gamma}}\right) \right], \quad (3.4)$$

where $\left(\frac{1}{\bar{\gamma}}\right) = \frac{|x_p^2 - \tilde{x}_p^2|}{\bar{\gamma}}$, $\left(\frac{1}{\bar{\gamma}}\right) = \frac{|x_r^1 - \tilde{x}_r^1|}{\bar{\gamma}}$, $\bar{\gamma}$ is the average SNR at each receive antenna and M is the number of iterations.

The unconditional PEP in (3.4) is substituted into (3.3) to get the final expression for (3.3).

3.4 Numerical Results

In this section, the numerical and analytical results for an $N_R \times N_T$ USTLD system, where $N_R = 4$ and $N_T = 2$ are presented for 16-QAM and 64-QAM. This section aims to verify the analytical framework developed in Section 3.3 how tight the simulation and analytical results converge; maximal ratio combining (MRC) reception is employed. Monte Carlo simulations have been carried out, where the BER is plotted per receive antenna against

SNR (dB). Performance comparisons for 16-QAM and 64-QAM were made at a BER value of 10^{-5} due to the long simulation period. Labeling mappers are demonstrated in Xu et al. [10]. Simulation parameters for the channels and AWGN are in line with those mentioned in Section 3.2. During simulation, we assumed that the channel is known at the receiver. The results in Figures 3.1 and Figure 3.2 illustrates that the simulation results are consistent with the analytical results at higher SNR regions.

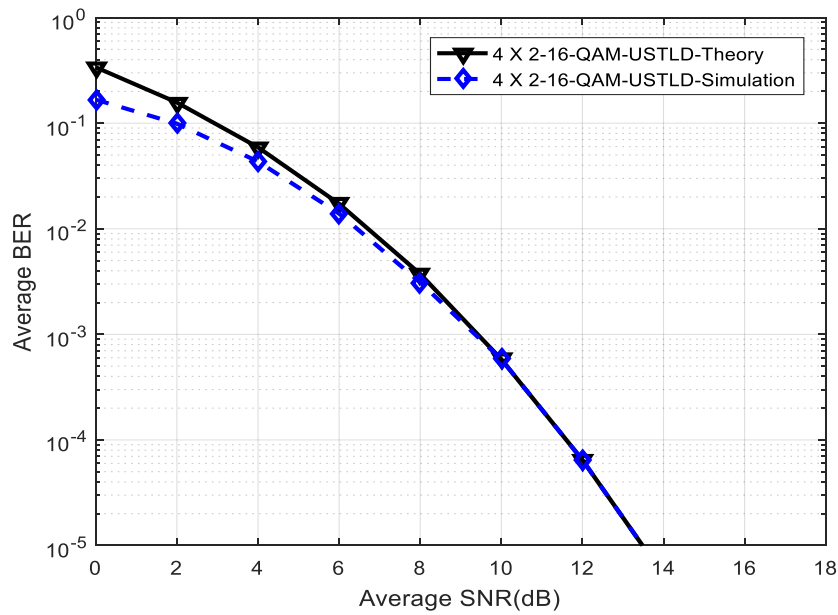


Figure 3.1: BER performance of the USTLD system for 16-QAM.

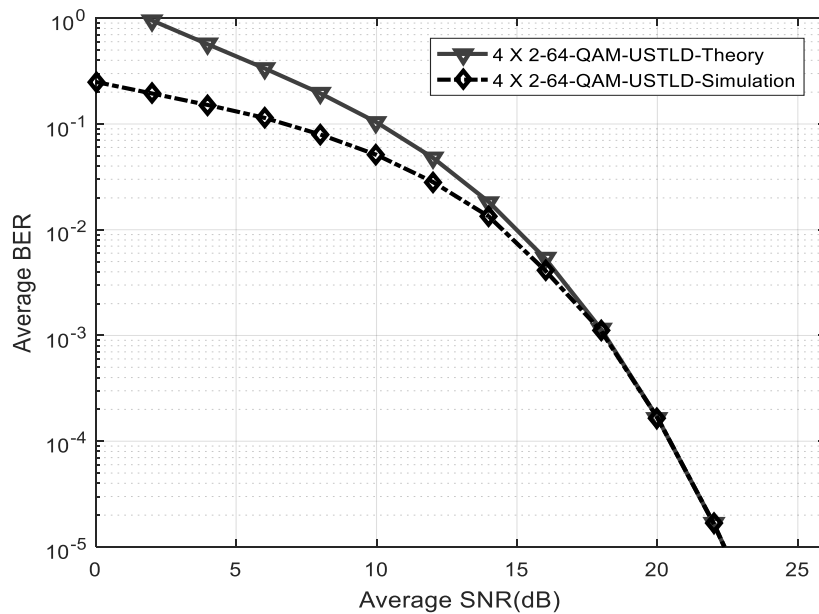


Figure 3.2 BER performance of the USTLD system for 64-QAM.

3.5 Conclusion

In this chapter, the USTLD technique was presented. The theoretical expression was derived using the union bound approach and perfectly correlated with the simulation results for 16-QAM and 64-QAM, respectively.

CHAPTER 4

A New Automatic Repeat Request Protocol Based on Alamouti Space-Time Block Code over Rayleigh Fading Channels

4.1 Introduction

Multiple-input multiple-output (MIMO) technique is employed in wireless networks to enhance the link reliability and/ or data rates [1]. MIMO systems achieve this by offering spatial multiplexing, spatial diversity, or a trade-off of both. Spatial multiplexing is accomplished with independent codewords sent to the receiver simultaneously, with the aim of improving data rates of wireless networks [2]. On the other hand, spatial diversity is realized by transmitting redundant codewords to the receiver to enhance link reliability. However, MIMO schemes have several disadvantages including high inter-channel interference (ICI), high proportion of radio frequency (RF) chains, high complexity for decoding due to ICI, high-energy efficiency and increased hardware costs because of multiple parallel transmitters and recipients [1]. There is also a trade-off regarding improved reliability and data rates. Consequently, extra protection regarding channel errors for the transmitted signal is necessary. Error management systems, such as automatic repeat request (ARQ) can be utilized to improve overall system error performance by offering additional robustness.

The ARQ protocol can be adopted into a MIMO system to improve diversity and error performance of the system by retransmitting the binary streams employing different symbol mapping in each transmission. ARQ protocol is a popular communications approach for improving the reliability of frames obtained in error through demanding retransmission [39].

MIMO based ARQ (MIMO-ARQ) schemes employing symbol mapping diversity (labeling diversity) have been studied to enhance the error performance of wireless communication systems [24, 25, 22]. In [24], Samra et al. proposed a MIMO-ARQ system employing symbol mapping for multiple packet retransmission using additive white Gaussian noise (AWGN).

The study by Samra et al. in [24] was later extended to fading channels, the system's diversity and error performance was improved by using symbol-mapping diversity among each retransmission [25]. Also, in [22], there is a published work in MIMO-ARQ. This scheme includes an incorporated receiver and mapping diversity, which significantly improves error performance by integrating a number of mapped transmissions into MIMO channels.

Alamouti scheme is another diversity technique that has the potential to improve the error performance and diversity in MIMO-ARQ wireless communication systems. The Alamouti scheme can achieve this by transmitting redundant duplicates of the original symbol to the receiver through two transmit antennas [35]. Alamouti MIMO-ARQ schemes in combination with MIMO communications were introduced for space-time coding. Onggosanusi et al. [40] proposed approaches of employing minimum mean squared error (MMSE) and zero-forcing (ZF) receivers to combine packet transmissions. In [41], a new hybrid automatic repeat request (HARQ) based on Alamouti STBC system was proposed. By using spatial and time diversity of MIMO channels, the approach improves the reliable HARQ packet transmission; it utilizes the pre-combining method and the Alamouti STBC full diversity to establish a reliable link. Simulation results indicate an improved error performance in the new system.

Motivated by the published work in [25, 22], a new automatic repeat request protocol based on Alamouti space-time block code over Rayleigh fading channels is introduced in this chapter. In [22, 25], results were presented for 16PSK and 16QAM employing flat fading channels. Labeling diversity is called mapping diversity in both systems in [22, 25]. The diversity between M retransmissions has been enhanced by adjusting the symbol mapping for every transmission. It was also noted that four transmit and four receive antennas were used in both techniques in [22, 25]. In addition, the study in [25], investigated mapping diversity on incoherent and coherent decoding with signal space diversity in flat fading channels. However, the proposed system does not employ flat-fading channels with coherent and incoherent and demodulation. This motivates an investigation of mapping diversity or labeling diversity in MIMO-ARQ systems over quasi-static Rayleigh fading channels. The proposed system also limits the system to two transmit antennas and four receive antennas.

4.2 Proposed System Model

Figure 4.1 displays the proposed system model with $N_T = 2$ transmit antennas and N_R receive antennas.

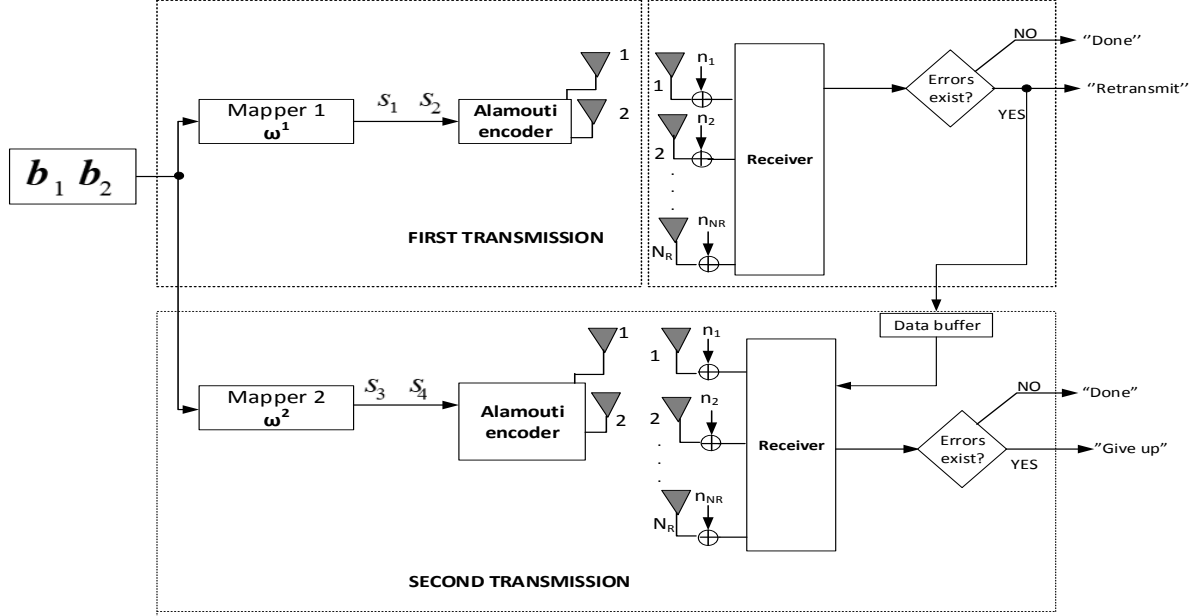


Figure 4.1: System model

The transmission is based on frames, where each frame has a length of $2N_o$ symbols and N_o is the maximum number of symbols in a frame. The proposed system considers two transmissions.

For the first frame, consider an $N_R \times N_T$ MIMO system, where $N_T = 2$ is the number of transmit antennas and N_R is the number of receive antennas. The binary streams $\mathbf{b}_1 = [b_{1,1} \ b_{1,2} \ \dots \ b_{1,m}]$ and $\mathbf{b}_2 = [b_{2,1} \ b_{2,2} \ \dots \ b_{2,m}]$, each of length $m = \log_2 M$, where M is the modulation order, are fed into mapper 1 (ω^1), which follows a Gray coded mapper, maps m bits into an M-QAM constellation points and yields symbols s_1 and s_2 . The two symbols are normalized such that $E\{|s_1|^2\} = E\{|s_2|^2\} = 1$. Then both symbols are fed into the Alamouti STBC encoder, to yield the STBC \mathbf{S}_{Alam} , denoted by:

$$\mathbf{S}_{Alam} = \begin{bmatrix} s_1 & s_2 \\ -s_2^* & s_1^* \end{bmatrix}. \quad (4.1)$$

At time slot one, the first and second antenna concurrently transmit symbols s_1 and s_2 ,

respectively. At time slot two, the first and second antenna concurrently transmit symbols $-s_2^*$ and s_1^* , respectively. The received signal vectors are expressed as:

$$\mathbf{y}_1 = \sqrt{\frac{E_s}{2}} (\mathbf{h}_1 s_1 + \mathbf{h}_2 s_2) + \mathbf{n}_1, \quad (4.2)$$

$$\mathbf{y}_2 = \sqrt{\frac{E_s}{2}} (-\mathbf{h}_1 s_2^* + \mathbf{h}_2 s_1^*) + \mathbf{n}_2, \quad (4.3)$$

where $\mathbf{y}_t \in \mathbb{C}^{(N_R \times 1)}$ denotes the t^{th} received signal vector for $t \in [1:2]$, E_s is the average SNR at each receive antenna. $\mathbf{n}_t \in \mathbb{C}^{(N_R \times 1)}$ and $\mathbf{h}_t \in \mathbb{C}^{(N_R \times 1)}$ signifies the t^{th} additive white Gaussian noise (AWGN) and the fading channel vector for $t \in [1:2]$. The complex entries of \mathbf{h}_t and \mathbf{n}_t are independent and identically distributed (i.i.d) Gaussian random variables (RVs) distributed as $CN(0,1)$. Furthermore, it is assumed that each entry of \mathbf{h}_t is quasi-static Rayleigh fading [15]. The channel remains the same value in two-time slots and takes an independent value in another two-time slots.

Based on [3, 32], it is assumed that the channel is known at the receiver. The received signals in (4.2) and (4.3) are sent to the combiner and the output of the combiner is given by:

$$r_1 = (\mathbf{h}_1^H)(\mathbf{y}_1) + (\mathbf{y}_2^H)(\mathbf{h}_2) = g_1 s_1 + \tilde{n}_1, \quad (4.4)$$

$$r_2 = (\mathbf{h}_2^H)(\mathbf{y}_1) - (\mathbf{y}_2^H)(\mathbf{h}_1) = g_1 s_2 + \tilde{n}_2, \quad (4.5)$$

where $g_1 = \sqrt{\frac{E_s}{2}} (\|\mathbf{h}_1\|_F^2 + \|\mathbf{h}_2\|_F^2)$, $\tilde{n}_1 = \mathbf{h}_1^H \mathbf{n}_1 + \mathbf{n}_2^H \mathbf{h}_2$ and $\tilde{n}_2 = \mathbf{h}_2^H \mathbf{n}_1 - \mathbf{n}_2^H \mathbf{h}_1$ [3, 33]. Furthermore, $\tilde{n}_1, \tilde{n}_2 \sim CN(0, \|\mathbf{h}_1\|_F^2 + \|\mathbf{h}_2\|_F^2)$ [3, 33]. Equations (4.4 – 4.5) can be further expressed as

$$r_\ell = g_1 s_\ell + \tilde{n}_\ell; \quad \ell \in [1:2], \quad (4.6)$$

Therefore, the estimation of the M-QAM symbols is done by minimizing the ML metric expressed as:

$$\hat{s}_1 = \operatorname{argmin}_{s_1 \in \mathcal{X}} (|r_1 - s_1|^2), \quad (4.7)$$

$$\hat{s}_2 = \operatorname{argmin}_{s_2 \in \mathcal{X}} (|r_2 - s_2|^2), \quad (4.8)$$

where χ is a set containing all the possible of modulated symbols, such that $\chi \cdot$

If there are errors from the first frame for χ symbols after detection, previous erroneous transmissions will be saved to the data buffer to minimize current transmission errors, typically by combining the ML detection of recent transmission. The transmitter will request a new transmission by transmitting the same binary streams \mathbf{b}_1 and \mathbf{b}_2 employing the second mapper (ω^2).

For the second frame, the binary streams \mathbf{b}_1 and \mathbf{b}_2 are fed into mapper 2 (ω^2), yielding the two symbols, s_3 and s_4 . The construction of the optimized labelling mapper, which ensures labeling diversity, includes solving a massive combination problem. The details on the construction of the optimized mappers for both 16-QAM and 64-QAM can be found in [10, 42]. We assume that $E\{|s_3|\} = E\{|s_4|\} = 1$. Afterwards, the symbols are fed into the Alamouti encoder. At time slot one, the first and second antenna concurrently transmit symbols s_3 and s_4 , respectively. At time slot two, the first and second antenna concurrently transmit symbols s_4 and s_3 , respectively. The received signals can be modelled as

$$\mathbf{y}_{t+1} = \mathbf{H}_1 \mathbf{s}_1 + \mathbf{n}_{t+1}, \quad (4.9)$$

$$\mathbf{y}_{t+2} = \mathbf{H}_2 \mathbf{s}_2 + \mathbf{n}_{t+2}, \quad (4.10)$$

where $\mathbf{y}_{t+2} \in \mathbb{C}^{(N_R \times 1)}$ is the t received signal vector for $t \in [1: 2]$, γ is the average SNR at each receive antenna. \mathbf{n} and \mathbf{n}_{t+2} are the AWGN vector and the fading channel vector for $[1: 2]$. The complex entries of \mathbf{H}_1 and \mathbf{n}_{t+2} are i.i.d Gaussian RVs distributed as $CN(0, \gamma)$. It is assumed that each entry of \mathbf{H}_1 is quasi-static Rayleigh fading [15]. The channel remains the same value in two-time slots and takes an independent value in another two-time slots.

Based on [3, 32], it is assumed that the channel is known at the receiver. The received signals in (4.9) and (4.10) are sent to the combiner and the output of the combiner is given by:

$$\tilde{\mathbf{n}}_3, \quad (4.11)$$

$$\tilde{\mathbf{n}} \quad (4.12)$$

where $g_2 = \sqrt{\frac{E_s}{2}} (\|\mathbf{h}_3\|_F^2 + \|\mathbf{h}_4\|_F^2)$, $\tilde{n}_3 = \mathbf{h}_3^H \mathbf{n}_3 + \mathbf{n}_4^H \mathbf{h}_4$ and $\tilde{n}_4 = \mathbf{h}_4^H \mathbf{n}_3 - \mathbf{n}_4^H \mathbf{h}_3$ [3, 33].

Furthermore, $\tilde{n}_3, \tilde{n}_4 \sim CN(0, \|\mathbf{h}_3\|_F^2 + \|\mathbf{h}_4\|_F^2)$ [3, 33]. Equations (4.11 - 4.12) can be further expressed as

$$r_{\ell+2} = g_2 s_{\ell+2} + \tilde{n}_{\ell+2}; \quad \ell \in [1:2], \quad (4.13)$$

Finally, the estimation of the M-QAM symbols is done by minimizing the joint ML metric expressed as:

$$[\hat{s}_1, \hat{s}_3] = \operatorname{argmin}_{s_1, s_3 \in \chi} (|r_1 - s_1|^2 + |r_3 - s_3|^2), \quad (4.14)$$

$$[\hat{s}_2, \hat{s}_4] = \operatorname{argmin}_{s_2, s_4 \in \chi} (|r_2 - s_2|^2 + |r_4 - s_4|^2), \quad (4.15)$$

where χ is a set containing all the possible of modulated symbols such that $s_1, s_2, s_3, s_4 \in \chi$.

4.3 Error Performance Analysis

In this section, we derive the theoretical analysis for the proposed scheme. The overall error probability of the system is formulated as:

$$P_e = P_a \times (1 - P_{e(\text{frame error})}) + P_b \times P_{e(\text{frame error})}. \quad (4.16)$$

where P_a is the symbol error probability for the first transmission, P_b is the symbol error probability for the second transmission and $P_{e(\text{frame error})}$ is the frame error probability.

The frame error probability can be found in [27] which is expressed by

$$P_{e(\text{frame error})} = \sum_{i=1}^{N_0} \binom{N_0}{i} P_c^i (1 - P_c)^{N_0-i}, \quad (4.17)$$

where N_0 is the maximum number of symbols in a frame. P_c is the symbol error probability of the symbols being successfully transmitted.

In the following sections, the symbol error probabilities are addressed separately for P_a and P_b .

4.3.1 Theoretical Analysis of P_a

In this section, we derive the symbol error probability for P_a , which is the theoretical analysis for the first transmission; the theoretical analysis is based on (4.6). The error probability for P_a is equivalent to the Alamouti system. In [34], the Alamouti system with N_R receive antennas has been confirmed to be equivalent to an MRC system with half SNR and $2N_R$ receive antennas.

The conditional pairwise error probability (PEP) for maximal ratio combining (MRC) has been formulated in [36, 35] and is expressed as:

$$P_{SEP}(\bar{\gamma}) = \frac{o}{n} \left[\frac{1}{2} \left(\frac{2}{\varpi\bar{\gamma}+2} \right)^{N_R} - \frac{o}{2} \left(\frac{1}{\varpi\bar{\gamma}+1} \right)^{N_R} + (1-o) \sum_{l=1}^{n-1} \left(\frac{S_l}{\varpi\bar{\gamma}+S_l} \right)^{N_R} + \sum_{l=n}^{2n-1} \left(\frac{S_l}{\varpi\bar{\gamma}+S_l} \right)^{N_R} \right], \quad (4.18)$$

where $S_l = 2\sin^2\left(\frac{l\pi}{4n}\right)$, $o = 4\left(1 - \frac{1}{\sqrt{M}}\right)$, $\varpi = \left(\frac{3}{M-1}\right)$, $\bar{\gamma} = \frac{E_s}{2}$ is the average SNR at each receive antenna and n is the number of iterations for $n > 10$.

Therefore, the symbol error probability (SEP) for P_a , is derived by replacing $\bar{\gamma}$ and N_R with $\frac{1}{2}\bar{\gamma}$ and $2N_R$ in (4.18). Hence, (4.18) becomes

$$P_{SEP}(\bar{\gamma}) = \frac{o}{n} \left[\frac{1}{2} \left(\frac{2}{\varpi\bar{\gamma}+2} \right)^{2N_R} - \frac{o}{2} \left(\frac{1}{\varpi\bar{\gamma}+1} \right)^{2N_R} + (1-o) \sum_{l=1}^{n-1} \left(\frac{S_l}{\varpi\bar{\gamma}+S_l} \right)^{2N_R} + \sum_{l=n}^{2n-1} \left(\frac{S_l}{\varpi\bar{\gamma}+S_l} \right)^{2N_R} \right], \quad (4.19)$$

4.3.2 Theoretical Analysis of P_b

In this section, we derive the theoretical analysis for P_b of the second transmission, which is the labelling diversity part. The theoretical analysis for P_b is based on the technique used in [10] and [42]. As indicated by Xu et.al [10], only one transmitted symbol pair is assumed to be detected with errors at high SNR, and the other transmitted symbol pair is correctly detected in the USTLD scheme. In this section, we assume that s_1 and s_3 are detected with errors while s_2 and s_4 are correctly detected. The theoretical expression for P_b is union bounded by [42]

$$P_b \leq \frac{1}{Mm} \sum_{p=0}^{M-1} \sum_{\substack{\hat{p}=0 \\ p \neq \hat{p}}}^{M-1} N(p, \hat{p}) P(\mathbf{S} \rightarrow \widehat{\mathbf{S}}). \quad (4.20)$$

In (4.20), $p = 1 + \sum_{\ell=1}^m 2^{m-\ell} \mathbf{b}_{1,\ell}$ is the symbol label, $P(\mathbf{S} \rightarrow \widehat{\mathbf{S}})$ is the pairwise error probability (PEP) of selecting the codeword $\widehat{\mathbf{S}}$ given that \mathbf{S} was transmitted, $\mathbf{S} = [s_1 \ s_3]$ and $\widehat{\mathbf{S}} = [\hat{s}_1 \ \hat{s}_3]$. $N(p, \hat{p})$ is the number of bit errors between the labels p and \hat{p} , $m = \log_2 M$ and M is the modulation order. The conditional PEP is expressed as:

$$P(\mathbf{S} \rightarrow \widehat{\mathbf{S}} | \mathbf{h}_1, \mathbf{h}_2, \mathbf{h}_3, \mathbf{h}_4) = P \left(\left| z_1 - \sqrt{\frac{E_s}{2}} g_1 \hat{s}_1 \right|^2 + \left| z_3 - \sqrt{\frac{E_s}{2}} g_2 \hat{s}_3 \right|^2 < \left| z_1 - \sqrt{\frac{E_s}{2}} g_1 s_1 \right|^2 + \left| z_3 - \sqrt{\frac{E_s}{2}} g_2 s_3 \right|^2 \right), \quad (4.21)$$

where $g_1 = (\|\mathbf{h}_1\|_F^2 + \|\mathbf{h}_2\|_F^2)$ and $g_2 = (\|\mathbf{h}_3\|_F^2 + \|\mathbf{h}_4\|_F^2)$. Substituting (4.6) and (4.13) into (4.21) yields:

$$P(\mathbf{S} \rightarrow \widehat{\mathbf{S}} | \mathbf{h}_1, \mathbf{h}_2, \mathbf{h}_3, \mathbf{h}_4) = P \left(\left| \sqrt{\frac{E_s}{2}} g_1 s_1 + \tilde{n}_1 - \sqrt{\frac{E_s}{2}} g_1 \hat{s}_1 \right|^2 + \left| \sqrt{\frac{E_s}{2}} g_2 s_3 + \tilde{n}_3 - \sqrt{\frac{E_s}{2}} g_2 \hat{s}_3 \right|^2 < \left| \sqrt{\frac{E_s}{2}} g_1 s_1 + \tilde{n}_1 - \sqrt{\frac{E_s}{2}} g_1 s_1 \right|^2 + \left| \sqrt{\frac{E_s}{2}} g_2 s_3 + \tilde{n}_3 - \sqrt{\frac{E_s}{2}} g_2 s_3 \right|^2 \right), \quad (4.22)$$

(4.22) can be simplified as:

$$P(\mathbf{S} \rightarrow \widehat{\mathbf{S}} | \mathbf{h}_1, \mathbf{h}_2, \mathbf{h}_3, \mathbf{h}_4) = P \left(\left| \sqrt{\frac{E_s}{2}} g_1 (s_1 - \hat{s}_1) + \tilde{n}_1 \right|^2 + \left| \sqrt{\frac{E_s}{2}} g_2 (s_3 - \hat{s}_3) + \tilde{n}_3 \right|^2 < |\tilde{n}_1|^2 + |\tilde{n}_3|^2 \right), \quad (4.23)$$

Treating the square as binomial and expanding likewise yields into:

$$P(\mathbf{S} \rightarrow \widehat{\mathbf{S}} | \mathbf{h}_1, \mathbf{h}_2, \mathbf{h}_3, \mathbf{h}_4) = P \left(\left| \sqrt{\frac{E_s}{2}} g_1 (s_1 - \hat{s}_1) \right|^2 + |\tilde{n}_1|^2 + 2Re \left\{ \sqrt{\frac{E_s}{2}} g_1 (s_1 - \hat{s}_1) \tilde{n}_1^* \right\} + \left| \sqrt{\frac{E_s}{2}} g_2 (s_3 - \hat{s}_3) \right|^2 + |\tilde{n}_3|^2 + 2Re \left\{ \sqrt{\frac{E_s}{2}} g_2 (s_3 - \hat{s}_3) \tilde{n}_3^* \right\} < |\tilde{n}_1|^2 + |\tilde{n}_3|^2 \right), \quad (4.24)$$

the expression in (4.24) can be further simplified as

$$P(\mathbf{S} = \hat{\mathbf{S}} | \mathbf{h}) = \left(A \left\{ \sqrt{E} \tilde{n}_1^* \right\} \left\{ \sqrt{E} \tilde{n}_3^* \right\} 0 \right), \quad (4.25)$$

where $\left| \sqrt{E} \hat{s}_1 \right|$, $\left| \sqrt{E} \hat{s}_2 \right|$, $\left\{ \sqrt{E} \tilde{n}_1^* \right\}$ and $\left\{ \sqrt{E} \tilde{n}_3^* \right\}$ are Gaussian random variables with zero mean and variances of $\left| \sqrt{E} \hat{s}_1 \right|$ and $\left| \sqrt{E} \hat{s}_2 \right|$. The total of these Gaussian random variables generates a new Gaussian random variable with zero mean and variance defined by: $\left| \sqrt{E} \hat{s}_1 \right| \left| \sqrt{E} \hat{s}_2 \right|$. We know that for a Gaussian random variable with zero mean and unit variance [43]

$$\frac{1}{\sqrt{2\pi}} \int_t \exp(-v^2) dv. \quad (4.26)$$

Therefore,

$$P(\mathbf{S} = \hat{\mathbf{S}} | \mathbf{h}) = \frac{\left| \sqrt{E} \hat{s}_1 \right| \left| \sqrt{E} \hat{s}_2 \right|}{\left(\sqrt{\left| \sqrt{E} \hat{s}_1 \right| \left| \sqrt{E} \hat{s}_2 \right|} \right)} \left(\sqrt{\frac{E_s}{|g_1|^2 |s_1 - \hat{s}_1|^2} + |g_2|^2 |s_2 - \hat{s}_2|^2} \right), \quad (4.27)$$

where Q is the Q-function, (4.27) can be expressed as:

$$P(\mathbf{S} \rightarrow \hat{\mathbf{S}} | \mathbf{h}_1, \mathbf{h}_2, \mathbf{h}_3, \mathbf{h}_4) = Q(\sqrt{\nabla_1 + \nabla_2}), \quad (4.28)$$

where $\nabla_1 = |g_1|^2 |s_1 - \hat{s}_1|^2$ and $\nabla_2 = |g_2|^2 |s_2 - \hat{s}_2|^2$ are central Chi-squared random variables with ν_1 and ν_2 degrees of freedom given by:

$$\nu_1 = 2 \left| \sqrt{E} \hat{s}_1 \right|^2, \quad \nu_2 = 2 \left| \sqrt{E} \hat{s}_2 \right|^2, \quad (4.29)$$

$$- |s \hat{ } | \Sigma , \quad (4.30)$$

where $\alpha_{1n}, \alpha_{2n} \sim N(0, \sigma_{\alpha\kappa}^2)$, with $\sigma = |s \hat{ }|^2$ and $= |s_3 - \hat{s}_3|^2$.

The probability density function (PDF) of [1 2] is indicated by [44]:

$$\frac{1}{(2 \kappa)} \exp\left(-\frac{\kappa}{2}\right). \quad (4.31)$$

The unconditional PEP is obtained by integrating the conditional PEP through the entire spectrum for and expressed by

$$P(\mathbf{S} \rightarrow \hat{\mathbf{S}}) = \int_0^\infty \int P(\mathbf{S} \hat{\mathbf{S}}|\mathbf{h}) , \quad (4.32)$$

substituting (4.28) into (4.32), yields

$$P(\mathbf{S} \rightarrow \hat{\mathbf{S}}) = \int_0^\infty \int_0^\infty Q(\sqrt{(\nabla_1 + \nabla_2)}) f \quad (4.33)$$

The integral in (4.33) is obtained by applying a trapezoidal approximation to the Q-function as revealed in [45]

$$-\left(\frac{1}{2} \exp\left(-\frac{c}{2}\right) + \sum_{i=1}^{n-1} \exp\left(-\frac{c}{2(-)}\right)\right), \quad (4.34)$$

where is the total number of iterations) [45]. Applying the parameter $\sqrt{\quad}$ into (4.34) yields:

$$Q(\sqrt{\quad}) = \left[- \left(-\frac{c}{2}\right) + \sum \left(-\frac{c}{2(-)}\right) \right]. \quad (4.35)$$

Substituting (4.36) into (4.34), results into

$$P(\mathbf{S} \hat{\mathbf{S}}) = \int_0^\infty \int \left[- \left(-\frac{c}{2}\right) + \sum \left(-\frac{c}{2(-)}\right) \right] f , \quad (4.36)$$

the expression in (4.36) can be expanded as

$$\begin{aligned}
P(\mathbf{S} \rightarrow \widehat{\mathbf{S}}) = & \\
& \int_0^\infty \int_0^\infty \frac{1}{2n} \left[\frac{1}{2} \exp\left(-\frac{\nabla_1}{2}\right) \exp\left(-\frac{\nabla_2}{2}\right) + \right. \\
& \left. \sum_{l=1}^n \exp\left(-\frac{\nabla_1}{2\sin^2\left(\frac{l\pi}{2n}\right)}\right) \exp\left(-\frac{\nabla_2}{2\sin^2\left(\frac{l\pi}{2n}\right)}\right) \right] f_{\nabla_1}(\nabla_1) f_{\nabla_2}(\nabla_2) d\nabla_1 d\nabla_2, \tag{4.37}
\end{aligned}$$

(4.37) can be simplified by employing the moment generating function (MGF) of the random variables, resulting in the following:

$$P(\mathbf{S} \rightarrow \widehat{\mathbf{S}}) = \frac{1}{2n} \left[\frac{1}{2} M_1\left(\frac{1}{2}\right) M_2\left(\frac{1}{2}\right) + \sum_{l=1}^{n-1} M_1\left(\frac{1}{2\sin^2\left(\frac{l\pi}{2n}\right)}\right) M_2\left(\frac{1}{2\sin^2\left(\frac{l\pi}{2n}\right)}\right) \right], \tag{4.38}$$

where $M_\kappa(\cdot)$ is the MGF of the random variables ∇_1 and ∇_2 defined as [44]

$$M_\kappa(s) = \int_0^\infty f_{\nabla_\kappa} \exp(-s\nabla_\kappa) d\nabla_\kappa = \left(\frac{1}{1+2\sigma_{\alpha_\kappa}^2 s} \right)^{2N_R}; \quad \kappa \in [1:2]. \tag{4.39}$$

The expression in (4.39) can be expanded as:

$$P(\mathbf{S} \rightarrow \widehat{\mathbf{S}}) = \frac{1}{2n} \left[\frac{1}{2} \left(\frac{1}{1+D_{s\hat{s}}} \right)^{2N_R} \left(\frac{1}{1+\tilde{D}_{s\hat{s}}} \right)^{2N_R} + \sum_{l=1}^{n-1} \left(\frac{1}{1+\frac{D_{s\hat{s}}}{S_l}} \right)^{2N_R} \left(\frac{1}{1+\frac{\tilde{D}_{s\hat{s}}}{S_l}} \right)^{2N_R} \right]. \tag{4.40}$$

In (4.41), $D_{s\hat{s}} = \frac{\bar{\gamma}}{8} |s_1 - \hat{s}_1|^2$, $\tilde{D}_{s\hat{s}} = \frac{\bar{\gamma}}{8} |s_3 - \hat{s}_3|^2$ and $S_l = \sin^2\left(\frac{l\pi}{2n}\right)$ and $\bar{\gamma} = \frac{E_s}{2}$ is the average SNR at each receive antenna.

Therefore, the unconditional PEP in (4.40) is substituted into (4.20) yielding the final expression for P_b .

Finally, equation (4.19) and (4.20) are substituted into (4.16) yielding the final expression for P_e .

4.4 Numerical Results

This section presents the numerical and theoretical results of an $N_R \times N_T$ new ARQ protocol based on Alamouti STBC over Rayleigh fading channels and Alamouti system where $N_R = 4$ and $N_T = 2$ are presented for 16-QAM and 64-QAM. This section aims to demonstrate the error performance gains for the proposed scheme when compared to the Alamouti system

under the same channel conditions, also compare the proposed system results when labeling diversity is employed or not employed and confirm the theoretical analysis established in Section 3.3. Monte Carlo simulations have been carried out, where the SEP is plotted per receive antenna against SNR (dB). Performance comparisons for 16-QAM and 64-QAM are made at a SEP value of 10^{-5} due to the long simulation period. Simulation parameters for the channels and AWGN are in line with those mentioned in Section 4.2. During simulation, we assumed that the channel is known at the receiver and the frame length is $2N_o$ symbols where $N_o = 100$. The Gray-coded and optimized labeling maps are illustrated in Figures A-1 and Figures A-2 for 16-QAM, and Figure A-3 and Figure A-4 for 64-QAM, respectively.

The results illustrated in Figure 4.2 and Figure 4.3 show that the proposed system exhibits an SNR performance gain of approximately 4 dB for 16-QAM and 4.90 dB for 64-QAM when one mapper is used as compared to the Alamouti scheme. However, it is noted from both results that when the proposed system uses two mappers, there is a significant gain of approximately 7.98 dB for 16-QAM and 9.8 dB for 64-QAM compared to the Alamouti system. The improved error performance is achieved from the secondary mapper introduced by the USTLD technique. Moreover, Figure 4.2 and Figure 4.3 also reveal that the theoretical expression results overlap with the simulation results in high SNR regions.

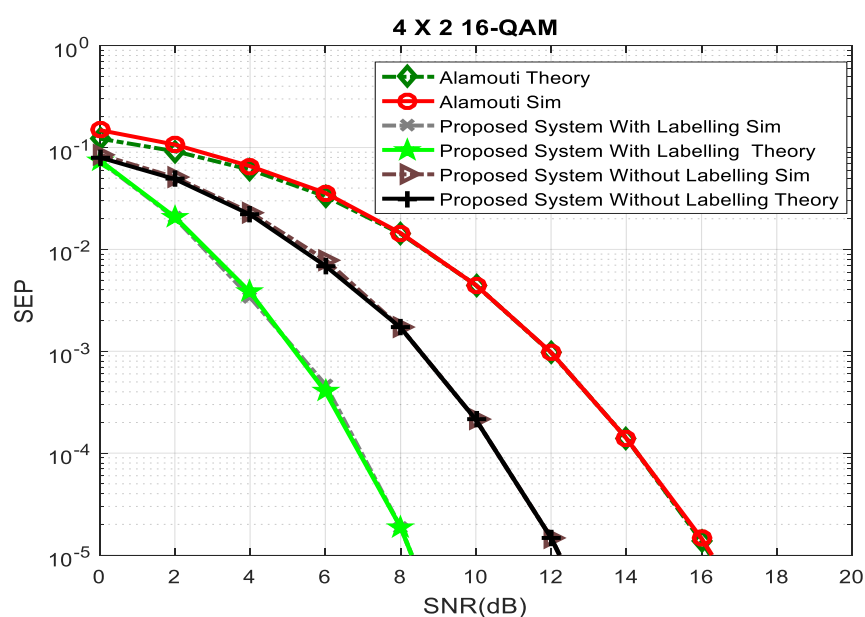


Figure 4.2: 4×2 16-QAM comparison of the proposed system and the Alamouti system.

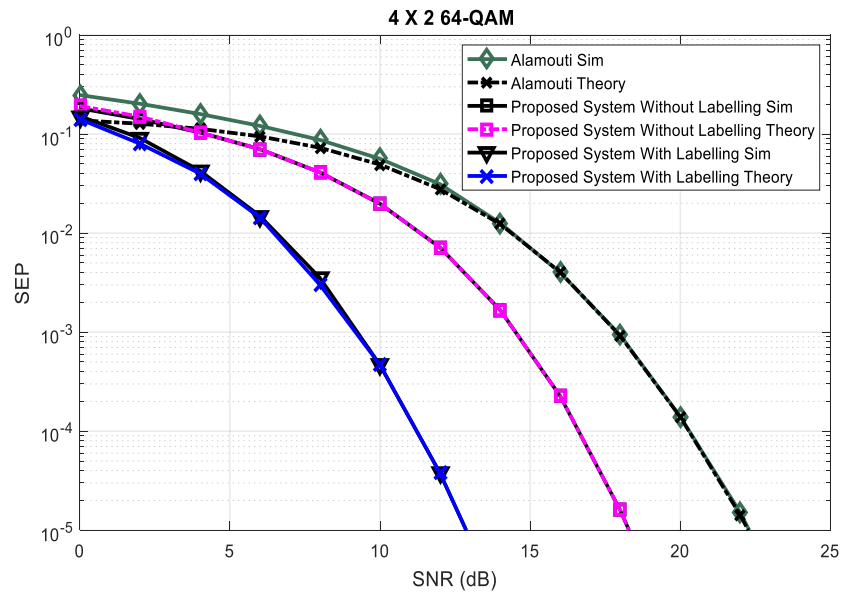


Figure 4.3: 4×2 64-QAM comparison of the proposed system and the Alamouti system.

Furthermore, results show that with the increase in modulation order the error performance improves. Multiple receivers and higher modulation orders mean more receive diversity as they increase the SNR at the destination. This, in turn, leads to an improved error performance [46]. This is because of the assumption that the theoretical analysis for P_b is obtained through the PEP technique for modulation order such as 64-QAM and therefore generate all possible error occurrences, overestimates the probability of error occurring at low SNR value. In addition, a codeword is very highly doubtful to really be decoded as the most improbable candidate in simulations at low SNR values. Such improbable candidates are higher in error, generated throughout the PEP bound; thus, further contributes to the overestimation of SEP at low SNR. Furthermore it can be noted from the results on the impact of retransmission, whereby the more you retransmit is the more the system improves in terms of error performance analysis.

4.5 Conclusion

In this chapter, a new ARQ protocol based on Alamouti STBC over Rayleigh fading channels was proposed for wireless communication systems. In addition, labeling diversity was employed in the proposed system to improve the error performance. To verify the simulation results, the theoretical expression was derived. The results revealed that there is a SEP performance improvement of approximately 4 dB for 16-QAM and 4.90 dB for 64-

QAM when one mapper is employed as compared to the Alamouti scheme at a SEP of 10^{-5} . The results also revealed that when the proposed system uses two mappers, there is a SEP performance improvement of approximately 7.98 dB for 16-QAM and 9.8 dB for 64-QAM as compared to the Alamouti system at a SEP of 10^{-5} .

CHAPTER 5

Conclusion and Future Research

This chapter highlights the contributions of the study and finally proposes future work regarding the work presented in this dissertation.

5.1 Concluding Remarks

In this dissertation, an automatic repeat request (ARQ) protocol in multiple-input multiple-output (MIMO) communication systems was investigated. The mathematical models, design methodology, and theoretical analysis were also developed.

The research contributions are provided below.

Firstly, an Alamouti transmission with ARQ protocol was investigated. The fundamental concept of the system was to incorporate Alamouti transmission to improve the error performance and data throughput by using two transmit antennas. The system only considered the first transmission ($N=1$) and second transmission ($N=2$). Furthermore, an error performance analysis on the symbol error probability (SEP) for the scheme employing M-ary quadrature amplitude modulation (M-QAM) over independent and identically distributed (i.i.d) quasi-static fading channels was derived and agree well with the simulation results. The approximate error performance gains for $N = 1$ and $N = 2$ is summarized in Table 5.1.

Modulation and configuration	Target SEP	$N = 1$	$N = 2$	Gain (dB)
16-QAM	10^{-5}	16.1	12.1	4
64-QAM	10^{-5}	22.4	17.5	4.90

Table 5.1: Summarized error performance gains of different number of transmission ($N = 1$ and $N = 2$) for various modulation schemes and orders.

Secondly, the uncoded space-time labeling diversity (USTLD) system was investigated. The theoretical expression was derived to validate simulation results. Simulation results were

performed for 4×2 USTLD scheme over i.i.d Rayleigh frequency-flat fading channels. In addition, the results presented were conducted for 16 QAM and 64-QAM and show that the theoretical expression results are consistent with the simulation results at high SNR regions.

Lastly, a new ARQ protocol based on Alamouti space-time block code over Rayleigh fading channels was proposed, which incorporates labelling diversity. Motivated by the error performance improvement advantages of the USTLD technique, it was employed in the system in Chapter 2 resulting on the proposed system in Chapter 4. In addition, the theoretical expression of the proposed system was derived over i.i.d quasi-static Rayleigh fading channels to validate the simulation results. Moreover, the simulation results for the proposed system were compared for the proposed system with labeling diversity, without labeling diversity and Alamouti system under the same channel assumptions.

The results revealed that there is a SEP performance improvement of approximately 4 dB for 16-QAM and 4.90 dB for 64-QAM when one mapper is employed as compared to the Alamouti system at a SEP of 10^{-5} . The results also revealed that when the proposed system uses two mappers, there is a SEP performance improvement of approximately 7.98 dB for 16-QAM and 9.8 dB for 64-QAM compared to the Alamouti scheme at a SEP of 10^{-5} . Furthermore, in all cases the theoretical expression developed of the proposed scheme match the simulation results at high SNR regions.

5.2 Future Research

The following aspects can be considered for investigation in future studies initiatives in addition to the work carried out in this dissertation:

- i. The proposed system used two transmit antennas and employed M-QAM modulation scheme. Future studies could be conducted for more than two transmit antennas and a comparative study could be investigated between M-ary phase shift keying (M-PSK) and M-QAM.
- ii. The proposed system could be investigated utilizing fading channel models, such as Rician fading channel models and Nakagami-m fading.
- iii. The proposed system could be implemented with differential space-time block codes (DSTBC) with a purpose of minimizing the power consumption of the system.

- iv. The delay of the system can be further investigated and the throughput of the proposed system.

APPENDIX A

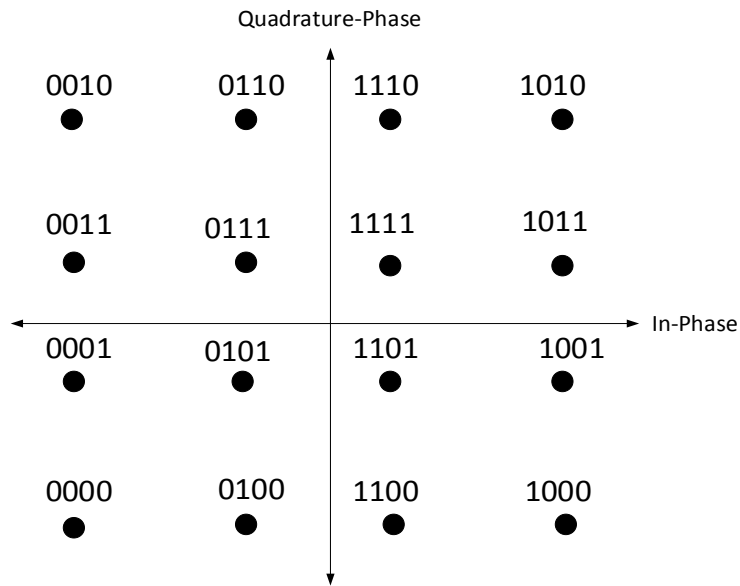


Figure A.1: 16-QAM Gray-coded labelling map (ω^1) [10, 43].

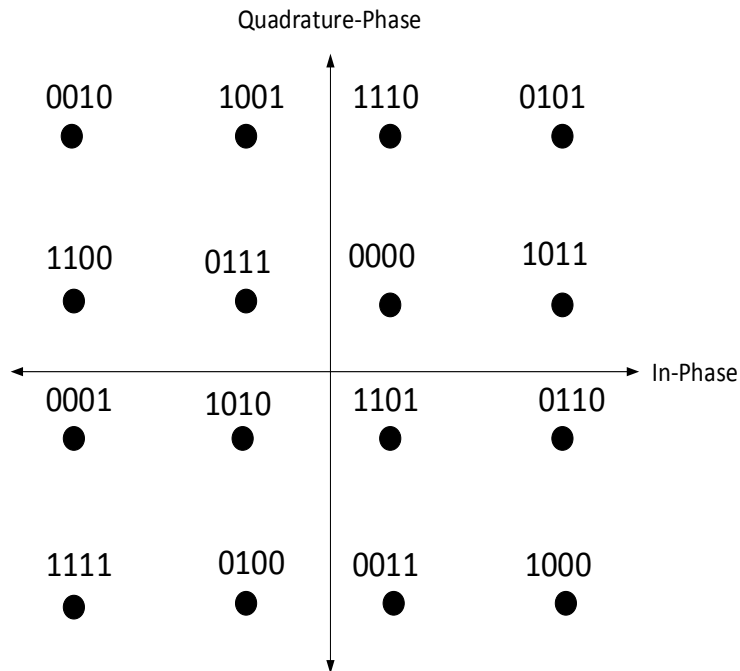


Figure A.2: 16-QAM optimized labelling map (ω^2) [10, 43].

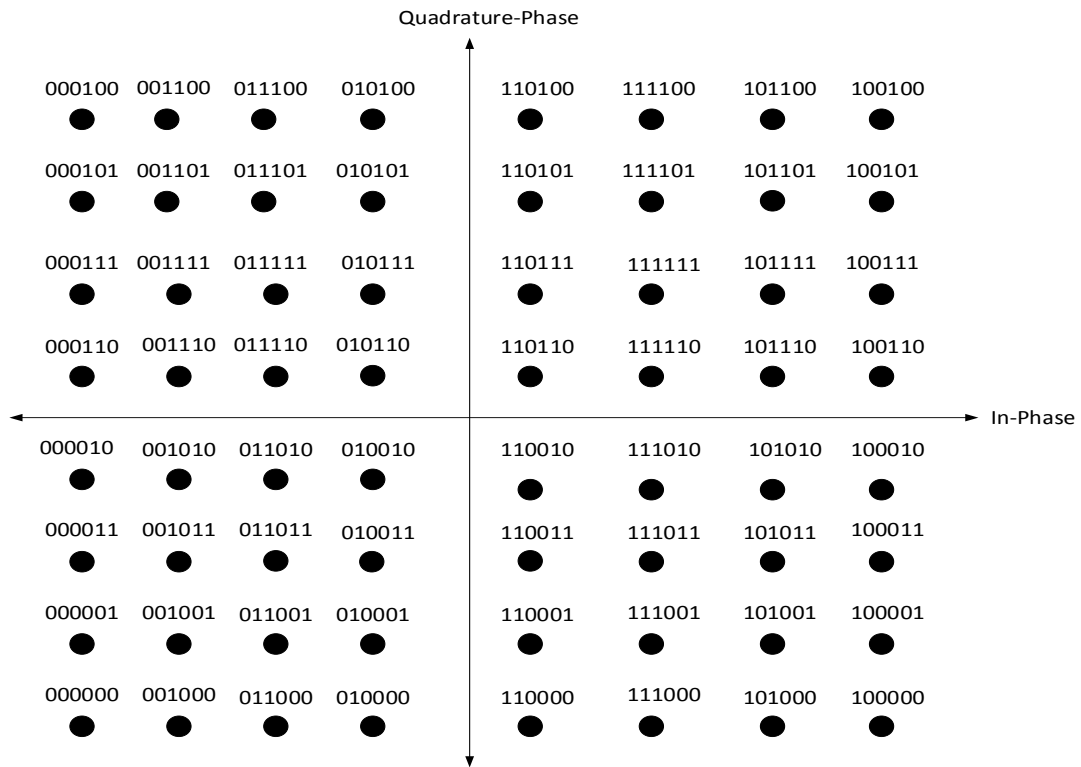


Figure A.3: 64-QAM Gray-coded labelling map (ω^1) [10, 43].

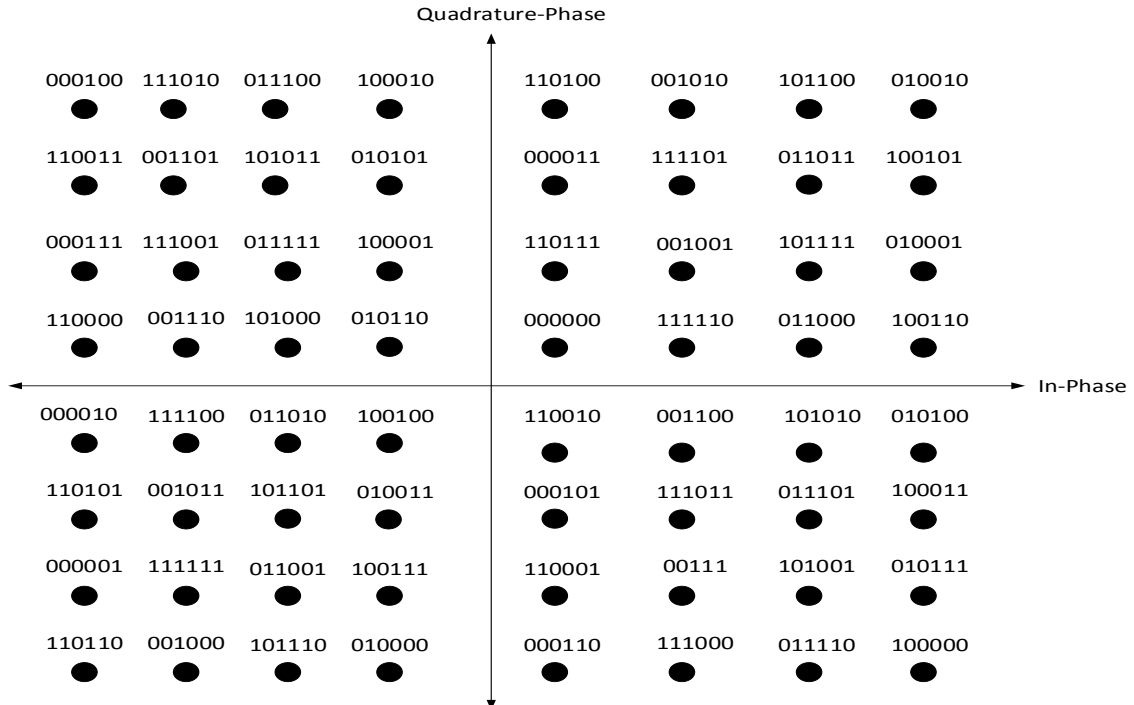


Figure A.4: 64-QAM optimized labelling map (ω^2) [10, 43].

REFERENCES

- [1] A. K. Afriyie, Multiple Input Multiple Output (MIMO) Operation Principles, Metropolia Ammattikorkeakoulu, Helsinki, Finland, 2013.
- [2] D. Gesbert, M. Shafi, D. Shiu, P. J. Smith and A. Naguib, "From Theory to Practice: An Overview of MIMO Space-Time Coded Wireless Systems," *IEEE Journal on Selected Areas in Communications*, vol. 21, no. 3, April 2003.
- [3] S. M. Alamouti, "A simple transmit diversity technique for wireless communications," *IEEE Journal on selected areas in communications*, vol. 16, no. 8, p. 1451–1458, October 1998.
- [4] H. Xu and N. Pillay, "Multiple Complex Symbol Golden Code," *IEEE Access*, vol. 8, pp. 103576-103584, doi: 10.1109/ACCESS.2020.2997308., 2020.
- [5] B. Vucetic and J. Yuan, Space-Time Coding Performance Analysis and Code Design : in Space-time Coding, John Wiley & Sons, 2003.
- [6] B. Guo, O. Sotoudeh, C. Zhou and Y. Cheng, "Antenna Diversity for a Mobile Terminal: Theory, Simulation and Measurement," in *GLOBECOM 2009 - 2009 IEEE Global Telecommunications Conference*, Honolulu, 2009.
- [7] Z. Hong and B. L. Hughes, "Robust space-time trellis codes based on bit-interleaved coded modulation," in *Conf. on Inform. Sc. and Sys. (CISS'01)*, March 2001.
- [8] H. Samra , Z. Ding and P. Hahn, "Symbol mapping diversity design for multiple packet transmission," *IEEE Trans Commun*, vol. 53, no. 5, p. 810-817, 2005.
- [9] K. G. Seddik , A. S. Ibrahim and K. J. Liu, "Trans-modulation in wireless relay networks," *IEEE Commun Lett*, vol. 12, no. 3, p. 170-173, 2008.
- [10] H. Xu, K. Govindasamy and N. Pillay, "Uncoded space-time labeling diversity," *IEEE communications letters*, vol. 20, no. 8, pp. 1511 - 1514, August 2016.

- [11] E. Akay, E. Sengul and E. Ayanoglu, "Achieving full spatial multiplexing and full diversity in wireless communications," in *Wireless Communications and Networking Conference WCNC 2006. IEEE*, 2006.
- [12] P. Babarczi, J. Tapolcai, A. Pašić, L. Rónyai, E. R. Bérczi-Kovács and M. Médard, "Diversity Coding in Two-Connected Networks," *IEEE/ACM Transactions on Networking*, vol. 25, no. 4, pp. 2308-2319, August 2017.
- [13] A. Goldsmith, *Wireless communications*, New York: Cambridge University Press, 2005.
- [14] C. Windpassinger, R. F. Fischer, T. Vencel and J. Huber, "Precoding in Multiantenna and Multiuser Communications," *IEEE Transactions on Wireless Communications*, vol. 3, no. 4, pp. 1305 - 1316, August 2004.
- [15] W. Yang, G. Durisi, T. Koch and Y. Polyanskiy, "Quasi-static multiple-antenna fading channels at finite blocklength," *IEEE Transactions on Information Theory*, vol. 60, no. 7, p. 4232–4265, July 2014.
- [16] B. Makki and T. Eriksson, "On the Performance of MIMO-ARQ Systems with Channel State Information at the Receiver," *IEEE Transactions on Communications*, vol. 62, no. 5, pp. 1588-1603, 2014.
- [17] S. Lin and D. J. Costello, *Error control coding: Fundamentals and applications*, Pearson-Prentice Hall, 2004.
- [18] K. Govindasamy, H. Xu and N. Pillay, "Space-time block coded spatial modulation with labeling diversity," *International Journal of Communication Systems*, vol. e3395, 2017.
- [19] P. W. Wolniansky, G. J. Foschini, G. D. Golden and R. A. Valenzuela, "V-BLAST: an architecture for realizing very high data rates over the rich-scattering wireless channel," *Signals, Systems, and Electronics*, pp. 295-300, 1998.
- [20] G. J. Foschini, "Layered space-time architecture for wireless communication in a fading environment when using multiple antennas," *Bell Labs Tech. J.*, vol. 1, no. 2, p. 41–59, 1996.

- [21] S. Zhihua , S. Haitong , Z. Chunming and D. Zhi , “Linear precoder optimization for ARQ packet retransmissions in centralized multiuser MIMO uplinks,” *Wireless Communications, IEEE Transactions*, vol. 7, no. 2, pp. 736-745, 2008.
- [22] H. Samra and Z. Ding, “New MIMO ARQ protocols and joint detection via sphere decoding,” *IEEE Transactions on Signal Processing*, vol. 54, no. 2, pp. 473-482, February 2006.
- [23] H. Samra and Z. Ding, “Sphere decoding for retransmission diversity in MIMO flat-fading channels,” in *IEEE International Conference on Acoustics, Speech, and Signal Processing*, 2004.
- [24] H. Samra, Z. Ding and P. M. Hahn, “Optimal symbol mapping diversity for multiple packet transmissions,” in *IEEE International Conference on Acoustics, Speech, and Signal Processing*, Hong Kong, 2003.
- [25] H. Samra, Z. Ding and P. M. Hahn, “Symbol mapping diversity design for packet retransmissions through fading channels,” in *IEEE GLOBECOM’03* , San Francisco, CA, December 2003.
- [26] H. Xiao and J. Ni, “Performance analysis of two-user cooperative ARQ protocol over Rayleigh fading channel,” *Journal on Wireless Communications and Networking*, January 2015.
- [27] S. Wicker, *Error Control Systems for Digital Communication and Storage*, Upper Saddle River (New Jersey): Prentice-Hall, 1995.
- [28] D. Chase, “Code combining—a maximum-likelihood decoding approach for combining an arbitrary number of noisy packets,” *IEEE Trans. Comm.*, vol. 33, pp. 385-393, 1985.
- [29] B. Harvey and S. Wicker, “Packet combining systems based on the Viterbi decoder,” *IEEE Trans. Comm.*, vol. 42, no. 3, pp. 1544-1557, 1994.
- [30] D. Rowitch and L. Milstein, “On the performance of hybrid FEC/ARQ systems using rate compatible punctured turbo (RCPT) codes,” *IEEE Trans. Comm.*, vol. 48, no. 6, pp. 948-

959, June 2000.

- [31] J. Hagenauer, "Rate-compatible punctured convolutional codes (RCPC codes) and their applications," *IEEE Trans. Comm.*, vol. 36, pp. 389-400, April 1988.
- [32] R. Hamila, M. O. Hasna and R. Bouallegue, "Modified Alamouti Decoding for Highly Selective channels for LTE systems," *IEEE ISSPA*, vol. 1, no. 1, pp. 140-144, 2012.
- [33] W. L. Ramasila and H. Xu, "Improved error performance of a 3/4-Sezginer space-time block codes," *International Journal for Communication Systems*, vol. 32, no. 13, 2019.
- [34] H. Xu, "Symbol error probability for generalized selection combining reception of m-qam," *SAIEE Africa Research Journal*, vol. 100, no. 3, p. 68–71, September 2009.
- [35] A. Saed, H. Xu a and T. Quazi, "Alamouti Space-time Block coded Hierarchical Modulation with Signal Space Diversity and MRC reception in Nakagami-m fading channels," *IET Communications*, vol. 8, no. 4, pp. 516-524, 2013.
- [36] A. Essop and H. Xu, "Alamouti Coded M-QAM with Single and Double Rotated Signal Space Diversity and generalised selection Combining Reception in Rayleigh Fading Channels," *SAIEE Africa Research Journal*, vol. 100, no. 3, pp. 221-223, 2015.
- [37] D. Ayanda , H. Xu and N. Pillay, "Uncoded M-ary quadrature amplitude modulation space-time labeling diversity with three transmit antennas," *Int. J. Commun. Syst.*, 2018:e3818. DOI: 10.1002/dac.3818..
- [38] Y. Huang and J. A. Ritcey, "Improved 16-QAM Constellation Labeling for BI-STCM-ID with the Alamouti Scheme," *IEEE Commun. Lett.* , vol. 9, no. 2, pp. 157-159, February 2005.
- [39] I. Stanojev, O. Simeone, U. Spagnolini, Y. Bar-Ness and R. L. Pickholtz, "Cooperative ARQ via auction-based spectrum leasing," *IEEE Trans. Commun.*, vol. 58, no. 6, p. 1843–1856 , 2010.
- [40] E. Onggosanusi, A. Dabak, Y. Hui and G. Jeong, "Hybrid ARQ transmission and combining for MIMO systems," in *IEEE International Conference on Communications* ,

May 2003.

- [41] K. Acolatse and Y. Bar-Ness, "An Alamouti-based Hybrid-ARQ Scheme for MIMO Systems," 2005. [Online]. Available: <https://www.eurasip.org/Proceedings/Ext/IST05/papers/347.pdf>. [Accessed 18 November 2020].
- [42] N. Pillay and H. Xu, "Uncoded space-time labeling diversity—application of media-based modulation with RF mirrors," *IEEE Commun Lett*, vol. 22, no. 2, p. 272-275, 2018.
- [43] K. Govindasamy, H. Xu and N. Pillay, "Space-time block coded spatial modulation with labeling diversity," *Int J Commun Syst*, 2017;e3395.<https://doi.org/10.1002/dac.3395>.
- [44] J. G. Proakis, "Probability and stochastic processes," in *Digital Communications*, New York, USA: McGraw-Hill, 2001.
- [45] Z. Paruk and H. Xu, "Performance analysis and simplified detection for two-dimensional signal space diversity with MRC reception," *SAIEE Africa Research Journal*, vol. 104, no. 3, pp. 97-106, September 2013.
- [46] S. Tarun, I. Kaur and B. Pahwa, "Simplified processing for high-efficiency wireless communication employing multiple antenna arrays," *IJCA*, vol. 87, no. 16, pp. 31 - 35, 2014.
- [47] M. Gidlund, "Design and performance of space-time block coded hybrid ARQ schemes for multiple antenna transmission," in *ISPACS*, February 2009.
- [48] S. Ejaz, F. Yang and H. Xu, "Labelling diversity for 2X2 WLAN coded networks," *Radio Engr.*, vol. 24, no. 9, p. 695-697, 2015.
- [49] M. Krasicki and P. Szulakiewicz, "Boosted space-time diversity scheme for wireless communications," *Electronics Lett.*, vol. 45, no. 16, p. 843-845, 2009.
- [50] M. Krasicki, "Essence of 16-QAM labelling diversity," *Electronics Letters*, vol. 49, no. 8, p. 567-569, 2013.

[51] Halim, E. Hartono and S. Soo-Young, "Improvement of BER performance of ALAMOUTI technique and IEEE 802.15.4 in MIMO system.," *Journal of the Internet Information Society for Korean Society for Internet Information*, vol. 14, no. 1, pp. 1-7, 2013.